Caesium Atomic Clocks: Function, Performance and Applications

Andreas Bauch

Physikalisch-Technische Bundesanstalt, Braunschweig, Germany
e-mail address: andreas.bauch@ptb.de

Abstract

For more than four decades, caesium atomic clocks have been the backbone in a variety of demanding applications in science and technology. Neither satellite based navigation systems, like the US Global Positioning System, nor the syntonization of telecommunication networks at the presently prescribed level would function without them. Recent years have brought major breakthroughs in the development, operation and mutual comparison of frequency standards based on the same hyperfine transition in caesium as used hitherto, but now incorporating the technique of laser cooling. Several cold-atom fountains have been developed. Mutual agreement within about one part in 10^{15} was demonstrated for two of them operated side by side but also for two operated simultaneously in the US and Germany. This paper gives a survey on currently available commercial caesium clocks and primary standards developed in national metrology institutes.

1. Introduction

The accurate measurement of time and frequency is vital to the success of many fields of science and technology. Examples from atomic physics are atom-photon interactions, atomic collisions, and atomic interactions with static and dynamic electromagnetic fields. Geodesy, radio-astronomy (very long baseline interferometry), and pulsar astronomy rely strongly on the availability of stable local frequency standards and uniform timescales. The same is valid for the operation of satellite-based navigation systems. However, more commonplace applications, such as management of electric power networks and telecommunication networks, also require synchronisation of local timing sources or syntonization of locally maintained frequency sources with national or international standards.

In almost all these fields atomic frequency standards (AFS) based on the caesium hyperfine transition at 9.2 GHz have played an important role since decades. Immediately after the demonstration of the first laboratory device in the National Physical Laboratory (NPL), UK, in 1955 (Essen and Parry 1957), a commercial variant, named Atomichron, was developed in the US in 1958 (Forman 1985). Today, hundreds of commercial caesium atomic clocks are

used in timing laboratories and in military and scientific centres. A brief discussion on principles, operation and characterization of AFS is given subsequently, followed by a description of the function of a caesium AFS. Section 4 includes the results of a survey on the performance of currently available caesium AFSs. *Primary frequency standards* or *clocks* are distinguished from the commercial clocks by the fact that the corrections due to *all* systematic frequency shifting effects can be estimated to the best of one's knowledge. The properties of today's clocks of this kind are summarized in section 5.

Using the technique of laser cooling, an improved type of caesium AFS has been developed during the last decade. The so-called fountain clocks have matured to be operated regularly and to contribute to the realization of International Atomic Time (Parker *et al* 2001, Weyers *et al* 2001). Their properties are dealt with in section 6, followed by a section dealing with the specific role of caesium clocks in the realization of International Atomic Time. After a quick glance on future developments the paper the paper is concluded with a summary.

Further details on the subject and in particular on rubidium AFS and the hydrogen maser can be found in the monographs of Gerber and Ballato (1984), of Major (1998), and of Riehle (2003). Vanier and Audoin (1989) explained the principles and the theoretical background in a very detailed fashion. Part of the material was previously published in Bauch and Telle (2002).

2 Atomic frequency standards: principle of operation and characterization of their performance

It is commonly assumed that atomic properties such as energy differences between atomic eigenstates and thus atomic transition frequencies are natural constants and do not depend on space and time (apart from relativistic effects). They are determined by fundamental constants which describe the interaction of elementary particles. A transition between two eigenstates differing in energy by ΔE is accompanied by absorption or emission of electromagnetic radiation of frequency $f = \Delta E/h$ (h: Planck constant). The principle of operation of a passive AFS is illustrated in figure 1. The choice of the particular atomic transition is directed by certain requirements. The first basic aim would be to minimise random fluctuations of the output signal, which requires that

(I) the natural linewidth $\Gamma^{(2)}$ of the transition is small,

(II) the interaction time T_i of the atomic absorber with the probing radiation is long,

[2] Γ is expressed as angular frequency throughout the text

(III) sources of probing radiation exist which deliver a spectrally narrow radiation so that no technical broadening of the observed resonance curve occurs,

(IV) the atomic resonance is observed with a high signal-to-noise ratio so that the statistical fluctuations of the signal I_D used for control of the LO are small.

If the first three criteria are fulfilled, in principle a narrow atomic resonance can be observed. Consider atoms being irradiated with a monochromatic radiation of frequency f_p during a time interval T_i. If Γ is sufficiently small, $\Gamma/(2\pi) << 1/T_i$, the observed line shape resembles the squared Fourier transform of the truncated sinusoidal waveform, and has a full width at half maximum (FWHM) of the order $0.9/T_i$.

The second basic aim would be to minimise systematic shifts of the realized output frequency f_r from that of unperturbed atoms. Two further requirements have been identified.

(V) The energy of the atomic eigenstates should be insensitive to electric and magnetic fields.

(VI) The velocity v of the probed atoms should be low.

Before we come back to these requirements in describing the function of a caesium clock, we briefly discuss the standard measures for the characterization of AFSs in general. The term *frequency instability* describes the stochastic or environmentally induced fluctuations of the output frequency of a standard. The frequency instability can be expressed in the time domain as a function of the measurement time τ (averaging time) or in the frequency domain by the power spectral density. A review of the measures is included in an ITU-Handbook (ITU 1997, sections 3 and 4). Levine (1999) has also given an excellent tutorial on the matter. Here we restrict ourselves to a widely accepted measure in the time domain which may characterize the AFS output. We consider normalized frequency differences $y(\tau)$ of the realized frequency from its nominal value or from a suitable reference, averaged over τ. The two-sample standard deviation $\sigma_y(\tau)$, introduced by Allan (1966), calculated according to

$$\sigma_y(\tau) = \left\{ \sum_{i=1}^{K-1} \left(y_{i+1}(\tau) - y_i(\tau) \right)^2 / (2K-2) \right\}^{1/2} \qquad (1)$$

is a useful measure of the relative frequency instability for an averaging time τ during the total measurement time $K \cdot \tau$, as long as $K \geq 10$ is valid. In a log-log plot of $\sigma_y(\tau)$ versus τ one can discriminate among some of the causes of instability in the clock signal because they lead to different slopes. If shot-noise of the detected atoms is the dominating noise source, the frequency noise is white and $\sigma_y(\tau)$ decreases with $\tau^{-1/2}$. In this case the use of $\sigma_y(\tau)$ is not

really mandatory because it agrees with the classical standard deviation of the sample. Typically, however, one notices long-term effects due to coloured noise processes which indicate that parameters defining f_r are not sufficiently well controlled. The classical standard deviation would diverge with increasing τ in such a case whereas $\sigma_y(\tau)$ remains bounded. The slope in the log-log plot then changes to zero or even becomes positive. The observed $\sigma_y(\tau)$ can be related with operational parameters of the AFS through the expression

$$\sigma_y(\tau) = \eta \,/\, \{\, Q\ (S/N)\cdot(\tau/\mathrm{s})^{1/2}\,\} \qquad (2)$$

In (2), η is a numerical factor of the order of unity, depending on the shape of the resonance line and of the method of frequency modulation to determine the line centre. Q is the line quality factor (transition frequency / FWHM), and (S/N) is the signal-to-noise ratio for a 1 Hz detection bandwidth. Equation (2) reflects the requirements (I)-(IV). Examples of instability diagrams are given in the following sections.

The term *accuracy* is generally used to express the depth of understanding and quantitative knowledge of all effects which may entail that the output of the AFS does not reflect the transition frequency of unperturbed atoms. The manufacturers of commercial clocks use the term in the specifications of the average clock frequency with respect to the SI second definition, but without giving details about the causes of potential frequency deviations. A detailed list of such causes is published for primary clocks, and examples of uncertainty budgets are given in sections 5 and 6. Here one expresses the lack of knowledge and estimates the *uncertainty u* due to individual effects. General rules how to do this are contained in an ISO Guide (ISO 1993).

3. Caesium atomic clocks, classical and optically pumped

Already in the early 1950s, the element caesium had been identified as a very suitable candidate to fulfil many of the above mentioned requirements. The reference transition is that between the F_g=4 and F_g=3 hyperfine ground-state energy levels in the isotope ^{133}Cs which, favourably, is the only stable isotope of this element. The indices g, and later on e, are used to distinguish ground-state from excited-state energy sublevels. Ground-state hyperfine transitions can be observed totally Fourier limited, (I) and (III) are fulfilled. Due to the relatively high vapour pressure at moderate temperatures T (e. g. about 400 K), intense thermal atomic beams can be generated easily. In favour of (VI), the mean thermal velocity, $\sim(T/M)^{1/2}$, where M is the atomic mass, is only about 200 m/s due to the large caesium mass and thus allows an interaction time T_i of a few milliseconds even in small structures. It has been more important, at least in the earlier days when the laser was still unknown, that

magnetic selection of caesium atoms in the different hyperfine states is possible, and that, at the same time, efficient detection of the atoms using surface ionization is achievable. In figure 2 the principle of a caesium atomic clock is shown. In such a "classical" caesium atomic clock a beam of atoms effuses from an oven and passes through the strong inhomogeneous magnetic field of a state-selecting magnet (polarizer). Depending on the atoms' effective magnetic moment the polarizer deflects atoms in different directions so that some of the atoms subsequently pass through the microwave cavity. These may be the atoms either in the states $F_g = 4$, $m_F = \#4$ and $F_g = 3$, $m_F = \#3, \#2,...,+3$, or in the states $F_g = 4$, $m_F = 4, 3,...,\#3$, depending on the chosen geometry. In a so-called Ramsey cavity, made up of an U-shaped waveguide, the atoms are irradiated twice with a standing microwave probing field of frequency f_p. Ramsey (1950, 1990) had shown that the interaction time T_i, as previously introduced, becomes equal to the time of flight between the two arms of the cavity. Transitions obeying the selection rules $\Delta F = \pm 1$, $\Delta m_F = 0$ can be induced. A second state-selecting magnet (analyzer) discriminates between atoms which have made a transition and those which have remained in the initial state and directs atoms in one of the states to a hot-wire detector. The atoms are ionized, and the ion current is processed to yield the control signal I_D. When f_p is tuned across f_r, I_D exhibits a resonance feature centred around f_r and shown schematically in figure 2b. In clock operation, the probing frequency is modulated around a central value, and by phase-sensitive detection of I_D and subsequent integration the control voltage U_R is generated which tunes the LO, a voltage-controlled, temperature-stabilized quartz oscillator, so that f_p and f_r agree on average. In commercial clocks, I_D is generated from the output of a secondary electron multiplier. This allows a rather fast modulation (usually sine-wave), and a time constant of the LO control loop of a few seconds is chosen. In primary clocks like those of the Physikalisch-Technische Bundesanstalt PTB square-wave frequency modulation at a rate of 4 Hz is used, and the time constant is 10 s or longer (Schröder 1991).

Described by the selection rules, seven microwave transitions exist which have a different frequency dependence on static magnetic fields. The atomic beam path is thus surrounded by a set of nested shields protecting against the Earth's magnetic field. A coil inside the shield generates a weak static magnetic field (traditionally named C-field) which shifts the transition frequencies for $m_F \neq 0$ linearly by 7 kHz$\cdot B \cdot m_F$,$\cdot$where B is the magnetic flux density in µT. It separates the resonance frequencies of the individual transitions by typically several hundred times the widths of the central fringe. Thus, in clock operation, the LO can be stabilized on the well resolved $m_F = 0 \rightarrow m_F = 0$ transition, which is shifted weakly by 0.0427 Hz$\cdot B^2$, B again in µT. Here we notice a first example of perturbations on the atomic energy states or on the detected line shape due to preparation, probing and detection of the

atoms. We continue with a brief list of further systematic shifts which occur in a caesium AFS, see Vanier and Audoin (1986) for full details.

The population (in terms of total number and mean velocity) of magnetic sublevels m_F behind the polarizer magnet is a function of m_F. Such a population imbalance may lead to various kinds of frequency shifts, like Rabi pulling (De Marchi *et al* 1984), Ramsey pulling (Cutler *et al* 1991), and those caused by Majorana transitions (Bauch and Schröder 1993). These shifts were found to impair the performance of commercial clocks, particularly those of older design.

Several velocity dependent shifts are known. We name Φ_1 (Φ_2) the phase of the first (second) interaction field in the cavity. The frequency of the central Ramsey fringe is shifted from its unperturbed value by

$$\delta f_\Phi = \langle\langle - (\Phi_2 - \Phi_1) / (2\cdot\pi\cdot T_i) \rangle_{tr} \rangle_{\rho(T)}, \qquad (3)$$

proportional to the atomic velocity v. Here $\langle..\rangle_{\rho(T)}$ denotes the average over the time-of-flight distribution of the atoms. In general, the field phase varies spatially in each interaction region and thus δf_Φ is slightly different for each atomic trajectory. Therefore, a trajectory averaging $\langle..\rangle_{tr}$ is indicated in (3). The finite conductivity of the cavity walls in conjunction with asymmetries (in length, in the surface properties) of the two arms of the cavity causes ($\Phi_2 - \Phi_1$) to deviate from zero. In commercial clocks, ($\Phi_2 - \Phi_1$) is minimized during manufacture of the cavity and is assumed to be constant over the operating time of the device. In primary clocks one determines δf_Φ during operation. The direction of the atomic beam can be reversed (see figure 6). After a beam reversal, the frequency shift should become $-\delta f_\Phi$ instead of δf_Φ. Successive operation with alternate beam directions allows the determination of δf_Φ and thus of the unperturbed line centre. The uncertainty in determining δf_Φ is mainly due to the imperfection of the beam retrace.

The frequency shift due to the quadratic Doppler effect, $\delta f_D = -f_r(v/c)^2/2$, is a consequence of the relativistic time dilation and therefore of the atomic velocity in the beam. To give examples, δf_D amounts to about $-3\cdot10^{-3}$ Hz for a Maxwell-Boltzmann velocity distribution in an atomic beam from an oven at about 400 K and $-5\cdot10^{-4}$ Hz in PTB CS2 due to a velocity selection process (section 5). A relative 10^{-14} clock uncertainty requires a determination of the centre of the 60 Hz to 100 Hz wide resonance line to $\approx 10^{-4}$ Hz (relatively $\aleph\ 10^{-6}$), which represents a technical and theoretical challenge. Sufficiently detailed knowledge of the line

shape is required. As δf_{Φ} and δf_D have different velocity dependencies (~v and ~v^2, respectively) both effects together shift and broaden the resonance line and make it asymmetric. If the velocity distribution is wide, the sum of the shifts shows a strong dependence on the amplitude of the microwave excitation field (Shirley *et al* 2001, Makdissi and de Clercq 2001). Due to magnetic state selection in commercial clocks the velocity distribution is narrower than the Maxwell-Boltzmann distribution. Nevertheless, several models of commercial caesium AFS were found to exhibit a significant sensitivity of the output frequency on ambient temperature and humidity, probably because of insufficient stabilization of the microwave power.

Interaction of the caesium atoms with the electric field of thermal radiation emitted from the vacuum enclosure reduces the clock frequency by about $1.6 \cdot 10^{-4}$ Hz at room temperature (Itano *et al* 1982, Bauch and Schröder 1997, Simon *et al* 1998) which is significant for primary clocks and fountains. The respective entries in tables 4 and 5 are related to the limited ability to specify the radiation field as that of a *perfect* black body at a well defined temperature.

Historically (Jones 2000, Nelson *et al* 2001), the measurement result of the hyperfine splitting frequency in caesium atoms made between 1956 and 1958 with the NPL caesium AFS with reference to the ephemeris second (Markowitz *et al* 1958), f_0 = 9 192 631 770 Hz, became the basis for the definition of the second in the International System of Units SI (BIPM 1998). The uncertainty of the NPL device was rated at 1 part in 10^{10}, thus the measurement uncertainty of 20 Hz was entirely that of the astronomical determination of the duration of the ephemeris second. Over the years, understanding of the causes of perturbations in caesium AFSs has been further improved and this, together with technological advances, has entailed a reduction of the clock uncertainty by almost three orders of magnitude in the best commercial devices (see table 2) and another factor of 20 in the best thermal beam primary clocks (section 5).

It is possible to replace the twofold magnetic selection by interaction with laser fields at a wavelength for example of the caesium D_2-line (λ = 852.1 nm). The relevant energy levels are depicted in figure 3. Excitation of the transition $F_g = 3$ [$F_g = 4$] $\Rightarrow$ $F_e = 3$ or 4 pumps the atoms into the hyperfine state $F_g = 4$ [$F_g = 3$] and allows state preparation of the atoms in one of the manifolds of hyperfine m_F sub-states. Excitation of the so-called cycling transition F_g=4 $\Rightarrow$ F_e=5 yields a larger number of fluorescence photons per atom as quantum mechanical selection rules allow radiative decay from the excited state only back to the initial ground state. It is therefore common to use this transition in the detection process. Optical pumping

and detection is employed in four primary clocks (see section 5) and has also been studied in a small AFS at the French Laboratoire d'Horloge Atomique (Petit *et al* 1992, Boussert *et al* 1997). Based on their studies, Tekelec Temex, France (www.temex.fr) is currently developing a commercial AFS (Baldy 1996). To the author's knowledge, series production has not yet begun, and no performance data can therefore be given in the following section. Clock development for the GPS-III program including optical pumping was recently reported (see below).

4. Commercial caesium clocks

Following the principles and ideas explained in the previous sections, caesium clocks have been produced commercially since the late 1950s. In designing these devices a compromise between weight, volume, power consumption, and performance and costs is unavoidable. Nowadays the clocks weigh about 25 kg and fit into 19-inch wide cabinets. Supply with AC and DC power at a typical rate of 50 W in parallel is common. Some models incorporate a battery for stand-alone operation for some ten minutes. To the author's knowledge, five manufacturers, enlisted in table 1 and in the following abbreviated by a single character, offer caesium clocks today. Manufacturers **A** and **D** offer several products for a wide range of applications. The specifications of products for general use have been compiled in table 2. **A** and **D** currently dominate the market of producing sealed caesium beam tubes (CBTs, see figure 2) and these are used to some extent in the products of **F** and **O**. Standard and high-performance versions of their clocks are offered. Part of the improved specifications of the latter is due to a larger atomic flux employed which entails a larger S/N ratio. The price to be paid (literally) is a faster depletion of the caesium reservoir and thus the more frequent need to replace the clocks' CBT.

Since the application of digital control processes has become state-of-the art, the performance of caesium clocks has improved considerably. In practically all devices, the control of the LO is periodically switched into an hold-over mode and several parameters affecting the accuracy and long-term stability of the clock are monitored. Among these are C field strength, the microwave field amplitude and the atomic flux (signal level) (Cutler and Giffard 1992). Operational parameters are logged and can be retrieved through a computer interface. Manufacturer **A** reported on the long-term performance as well as on the statistics of the CBT operating times, with emphasis on clocks operated in US time-keeping institutes (Kusters *et al* 1999). Data concerning the accuracy and long-term stability of the ensemble of clocks operated in the time-keeping laboratories world-wide is included in section 7. Subsequently we give examples of the observed frequency instability of clocks operated at

PTB in laboratory environment. In figure 4 records of the short-term frequency instability of one clock are shown, one taken at an early time of operation and the other one a few months before the CBT ran out of caesium. The new tube yields a slightly more stable signal, specifications, however, were fulfilled at all times. The long-term behaviour of two clocks is illustrated in figure 5, using data over one year. The frequency instability is to a large extent governed by white frequency noise ($\sim \tau^{-1/2}$) up to the longest averaging times studied here.

Applications in the telecommunication sector require specialized output signals and thus additional features. Recommendation ITU-T G.801 of the International Telecommunication Union specifies that the rate of the Primary Reference Clock (PRC) of a nation-wide network must not deviate from the rate of TAI, at all times, by more than $\pm 10^{-11}$, relatively. The use of caesium clocks is one choice for a PRC. Manufacturer **O** offers his clock as part of a unit generating a range of specific telecommunication signals. The naked clock is apparently no longer offered, as it had been the case a few years ago. The description of some features is very similar with to of product **D**-4065. The specified accuracy, however, is worse by a factor of 5 and no further specifications could be obtained. Manufacturer **D** also offers specific telecommunication products probably based on CBT included in the standard products.

Manufacturers **D** and **F** offer caesium clocks with stringent detailed specifications for applications in adverse environment (magnetic field, outside pressure, shock, acceleration, ionizing radiation, according to MIL standards). For details, the reader is referred to the points of contact given in table 1.

Today's global navigation satellite systems would not function without the operation of caesium AFS in the ground segment and in many of the satellites. Numerous papers on experimentation, operation and properties of the space clocks of the US Global Positioning System GPS were published over the years in the Proceedings of the Annual Precise Time and Time Interval Systems and Applications Meeting. We briefly summarize the current status. The older block II and block IIA satellites carry two caesium and two rubidium AFS. In total 46 caesium AFS were launched, 41 supplied by **D**, 3 by **K** and 2 by **F**. The performance of some of these clocks was discussed by Mc Caskill *et al* (1999) and Wu and Feess (2000). Some clocks have functioned in space for 10 years and more. The typical relative frequency instability at τ = 1 day is of order $1 \cdot 10^{-13}$. Three caesium clocks are on board of Russian GLONASS (Global Navigation Satellite System) satellites. They were developed by the Russian Institute of Radionavigation and Time, St. Petersburg. The clocks' performance is typically inferior to that of GPS clocks. The relative frequency instability at τ = 1 day was

reported as about $5 \cdot 10^{-13}$. A serious drawback is their very short operational time in space, of typically less than 2 years (Bassevich *et al* 1996).

As operational lifetime and short-term frequency instability (up to a few hours) are the key parameters for space clocks in navigation systems, rubidium AFS have been used since many years. The GPS block IIR satellites which are launched in replacement of older satellites since 1997 carry three rubidium AFS only. According to Wu and Feess (2000), three digital caesium AFS will again be used onboard the future GPS block IIF satellites. Other information says that block IIF satellites will be equipped with one caesium and two rubidium clock. Development of an optically pumped caesium AFS for the GPS-III program was recently presented by Lutwak *et al* (2002). The current design of the future European navigation system Galileo specifies one passive hydrogen maser and two rubidium AFS onboard the Galileo satellites.

5. Primary clocks

In the mid of 2002, two “classical” primary clocks, CS1 and CS2 of the Physikalisch-Technische Bundesanstalt, are continuously operated and serve, among other standards which are mentioned below, as long-term references for the realization of International Atomic Time (section 6 of ITU (1997), Bauch *et al* (1998, 2000)). Four-pole and six-pole *magnets* (”magnetic lenses”) are used for state selection and velocity selection in these devices. In consequence, the mean atomic velocity is more than a factor of two lower than in an effusive thermal beam from the same source, and atomic velocities are confined in a narrow interval around the mean velocity. This proved advantageous to obtain a small uncertainty (Audoin 1992). A sketch of the CS2 design is shown in figure 6. Figure 7a) shows the CS2 "clock signal". About $1.3 \cdot 10^{7}$ atoms s^{-1} in a thermal atomic beam of about 95 $m \cdot s^{-1}$ mean velocity contribute to the signal. The CS2 interaction time amounts to about 10 ms, and the resonance curve of 60 Hz width is recorded with a *S*/*N* of 1000 in 1 Hz bandwidth. The largest systematic frequency shift, due to a magnetic field present in the interaction region, is as large as 2.92 Hz (relative shift $\aleph$ $3 \cdot 10^{-10}$), but like all other shifts it can be so well determined that in the mid-1980s u(CS2) could already be estimated as $15 \cdot 10^{-15}$ (Bauch *et al* 1988).

Optical preparation and detection is employed in four primary standards which were operated during recent years, CRL-01 of the Japanese Communications Research Laboratory (Lee *et al* 1999, Hasegawa *et al* 2000), the French JPO (Jet de Pompage Optique) (Makdissi and de Clercq 2001), developed at the Laboratoire Primaire du Temps et des Fréquences, NIST-7 of the US National Institute for Standards and Technology (Lee *et al* 1995, Shirley *et al* 2001),

and NRLM-4 of the Japanese National Research Laboratory of Metrology (Hagimoto *et al* 1999). NRLM changed its name meanwhile to National Metrology Institute of Japan (NMIJ) and is part of the National Institute of Advanced Industrial Science and Technology (AIST). CRL-01 practically is a duplicate of NIST-7 and was developed in collaboration of the two institutes. Parameters characterizing the performance and the uncertainty budget of the clocks are compiled in tables 3 and 4, respectively. Data were taken from the references given above. The $\sigma_y(\tau)$ – values of the clocks, which have almost the same line *Q*, differ considerably. This is in part due to the advantage of using optical *state preparation* rather than *state selection*. On the other hand, the S/N ratio is also dictated by the admitted caesium consumption. A 5 g caesium charge in each of the two CS2 ovens has been sufficient to operate CS2 from 1986 until now without interruptions of more than some ten hours. If one had aimed at a fivefold S/N ratio a 25-fold caesium consumption was required, which is prohibitive for clock operation. The caesium consumption in the JPO was reported to be 3 g per year (Makdissi and de Clercq 2001), explaining the large S/N. In figure 7 b) the JPO clock signal is depicted. Due to the wide thermal velocity distribution the Ramsey interference fringes are smeared out except of the central ones, and the fringe contrast is reduced. The width of the central feature is about 100 Hz.

To conclude this section, primary clocks with a thermal atomic beam currently permit the realization of the SI second with a relative uncertainty of the order of one part in 10^{14}. Their importance in the realization of International Atomic Time TAI is explained in section 7. Criteria (I), (III) - (V) of section 2 are essentially fulfilled for these clocks. A substantial step towards a better fulfillment of criteria (II) and (VI) has been possible only by using laser cooled atoms in a fountain design.

6. Caesium AFS based on laser cooled atoms: the atomic fountain

Already in the mid–1950s, even before the development of the first commercial caesium clock was completed, Jerome Zacharias at the Massachusetts Institute of Technology, USA, envisaged a device in which sufficiently slow atoms from a thermal atom source, directed vertically upwards, would stop and descend under the action of gravity and would provide an interaction time T_i of more than one second (Forman 1985, Naumann and Stroke 1995). Whereas this attempt was not successful because of the loss of the very slow atoms due to collisions, laser cooling has enabled the realization of such an atomic fountain clock in the last decade. Here we do not explain laser cooling but refer to the extensive literature, like the 1997 Nobel lectures (Chu 1998, Cohen -Tannoudji 1998, Phillips 1998). The principles have also been laid down in Letokhov *et al* (1995) and Metcalf and van der Straaten (1999). Part of a fountain is a so-called optical molasses (Chu *et al* 1985) which - in an intuitively simple

configuration - consists of three pairs of mutually orthogonal laser beams. The laser frequency is detuned to the red of a cyclic transition (2 in figure 3), essential for cooling, and the polarization vectors of the laser beams are in general mutually orthogonal. In addition, radiation which drives a pumping transition is superimposed to at least one of the beams. In the intersecting volume of the lasers the motion of atoms is severely damped and is like that of particles in a viscous fluid. The attainable kinetic energy of the random atomic motion in the molasses is expressed by a temperature. Low temperatures of a few Mikrokelvin can be achieved for some kinds of atoms. Among those is caesium for which typically about 2 µK is achieved, corresponding to a (random) velocity of 11 $mm \cdot s^{-1}$.

A molasses is not a *trap* in which a restoring force would attract atoms towards a certain point in space. However, if an inhomogeneous magnetic field is superimposed on a molasses, the Zeeman effect shifts the atomic levels depending on the atom's position. If the polarisation of the laser beams is adequately chosen a restoring force towards the zero-field point, preferentially located at the molasses centre, is created, in addition to the damping forces (Raab *et al* 1987). Such a magneto-optical trap (MOT) is sometimes used in fountains in order to facilitate the rapid loading of a sufficiently large number of atoms from a background vapour, followed by a pure molasses cooling step (magnetic field off) which then leads to the low temperatures mentioned above.

Achieving low temperatures is of utmost importance for the following reason. Trapping and cooling of atoms are connected with strong shifts of the hyperfine energy states, and precision spectroscopy becomes impossible. Therefore the cooled atoms have to be released and then the cloud of cold atoms expands corresponding to its temperature. Instead of just letting the atoms fall under the action of gravity, they are launched upwards and the microwave excitation is performed during a ballistic flight. The so-called moving molasses technique is used for the launching (Clairon *et al* 1991). It is most conveniently described for the six-laser-beam configuration with one pair of lasers directed vertically. The frequency of the laser light directed downwards is further decreased by δf_L, and that of the upwards-directed light is increased by the same amount. The atoms are thus exposed to a "walking wave" where the nodes and antinodes of the light field walk with velocity $v_S = \lambda \cdot \delta f_L$. Laser cooling is continuing in the moving frame and the atoms' initial low temperature is not increased. Atoms are accelerated to v_S within about 1 ms. When the laser fields are switched off at that instant, atoms continue to move on ballistic trajectories and come to rest under the action of gravity at a height of $H = v_S^2/(2 \cdot g)$. If H is adjusted to 1 m ($v_s = 4.4\ m \cdot s^{-1}$), then the total time of flight, back to the starting point, is about 0.9 s.

A fountain clock is operated in a pulsed mode, which is illustrated in figure 8. After launch, the atoms interact twice with the field sustained in the microwave cavity on their way up and on their way down. The interaction time T_i becomes as large as 0.5 s. The detection comprises the determination of the number of atoms $N_{at} := N_3 + N_4$ in both hyperfine levels, F_g=3 and F_g=4. The transition probability is then determined as $p_{34} = N_3 / N_{at}$ - in case where the atoms had been initially prepared in the F_g=4 level - and becomes independent of the cycle-to-cycle fluctuation of the number of launched atoms. During clock operation, p_{34} is determined changing the frequency f_p from cycle to cycle alternately on either side of the central fringe where the sensitivity to changes of f_p relative to f_r has its maximum. The difference of successive measurements is numerically integrated and a control signal is derived to steer the LO or to adjust the output frequency of a synthesizer included in the generation of the microwave signal.

Following initial work at the Ecole Normale Superieur (Clairon *et al* 1991), the first device of that kind, FO1, was developed at the LPTF (Clairon *et al* 1995). Its relative uncertainty u was initially estimated to be $3 \cdot 10^{-15}$ and later reduced to $1.1 \cdot 10^{-15}$ (Clairon *et al* 1996, Lemonde *et al* 2001). Up to mid 2002, frequency data and uncertainty evaluations have been published for two other caesium fountains, NIST-F1 (Jefferts *et al* 1999, Meekhoff *et al* 2001) and CSF1 of PTB (Weyers *et al* 2001). In figure 9 the CSF1 set-up with the basic constituent parts is depicted. A record of the (4,0)-(3,0) clock transition is shown in figure 10. In table 5, the uncertainty budgets for the three fountains are given. The entries appear quite similar. Because of the reduced linewidth, somewhat below 1 Hz, and the reduced atomic velocity some systematic frequency shifting effects are reduced by orders of magnitude compared with the entries in table 4. A new frequency shifting effect needs consideration when ultra-cold atoms are used in a frequency standard. The cross section for frequency-shifting collisions becomes much larger than that of thermal atoms of the same species. The collisional shift is proportional to the density of atoms in the cloud and depends on details of the atomic state in which the atomic cloud has been initially prepared. As obvious from table 5, the collisional frequency shift currently leads to the limiting uncertainty contributions and is still a subject of detailed studies.

The discussion of the frequency instability addresses a problem common to fountain frequency standards and beam standards. In all devices the LO is servo-controlled to the centre of the reference resonance. For this purpose, the probing frequency is periodically modulated and the output signal of the atomic resonator (see figures 1 and 2) is synchronously demodulated. Thus, the gain of the servo control is a periodic variable function of time and may become zero. This is straightforward to see for a fountain in which

the loading time constitutes such a zero-gain period. One can show that the apparently continuously available control signal in a beam standard is also deficient of information on the LO phase excursions twice during each modulation period for time intervals of typically a few times T_i (Audoin *et al* 1991). In all cases, the frequency noise of the LO at Fourier frequencies equal to even multiples of the modulation frequency is transposed to the quasi-DC control voltage. It constitutes a noise source in addition to, e.g., atomic shot noise. Historically, this aliasing phenomenon has been known from sampling theory, and its importance in passive frequency standards was early pointed out by Kramer (1974). It became of increased relevance when very low frequency instabilities had been reached in trapped ion microwave frequency standards (Dick 1987, Dick *et al* 1990). Nowadays the term *Dick effect* has become common usage. Audoin *et al* (1998) and Santarelli *et al* (1998) treated it quantitatively. The relative frequency instability of FO1 is about $1.5{\cdot}10^{-13}{\cdot}(\tau/\mathrm{s})^{-1/2}$, deteriorated by the Dick effect. It could be reduced by a factor of 4 when an ultra-stable LO was employed (Luiten *et al* 1995, Santarelli *et al* 1999). In the other fountains lower atom densities are used and the Dick effect is thus less decisive. The CSF1 instability is about $2.5{\cdot}10^{-13}{\cdot}(\tau/\mathrm{s})^{-1/2}$ and a somewhat higher value was reported for NIST-F1.

At LPTF, FO1 was compared during many months with a second fountain clock, named PHARAO (see section 8). Lemonde *et al* (2001) reported agreement between the two devices to better than $1{\cdot}10^{-15}$. NIST-F1 and CSF1 were compared using two high precision transfer techniques. Continuous frequency comparisons between the time scale UTC(NIST) and a hydrogen maser (HM) at PTB were performed using geodetic GPS receivers operated at NIST and PTB (Nelson *et al* 2000). In parallel, Two-Way Satellite Time and Frequency Transfer (TWSTFT) via a geostationary telecommunication satellite was employed (Bauch and Telle 2002). Thus, UTC(NIST) and the maser at PTB served as intermediate frequency references for the comparisons of NIST-F1 and CSF1. In Fig.11 the evaluated frequency differences are compiled (Parker 2002).

7. The role of caesium clocks in the realization of TAI

The realization of TAI has been the responsibility of the Bureau International des Poids et Mesures (BIPM) under the authority of the Comité International des Poids et Mesures (CIPM) (section 6 of ITU 1997). Data can be found at http://www.bipm.org/enus/5_Scientific/c_time/time_ftp.shtml in several subdirectories. The BIPM Time Section collects and processes time comparison data obtained using different techniques from about 50 timing centres world-wide. They represent mutual comparisons of 200 atomic clocks operated in the timing centres. Commercial caesium clocks to the largest part, a few hydrogen masers and very few primary clocks form the clock ensemble. In a first

step, a free atomic time scale, EAL (Echelle Atomique Libre), is produced using an iterative algorithm. The algorithm was designed to achieve a good long-term stability and high reliability of EAL. It assigns statistical weights to each contributing clock which are inversely proportional to a variance measuring the clock instability. To ensure reliability, the weights cannot go above a certain maximum (Thomas and Azoubib 1996). The distribution and temporal evolution of the statistical weights in 2001 is illustrated in figure 12.

The duration of the scale unit of EAL is determined with reference to primary clocks which realise the SI second with a specified uncertainty. During recent years, data were available from the clocks and fountains mentioned in sections 5 and 6, except FO1. A linear function of time is added to the EAL and the new scale is named TAI. The slope of this function is chosen so that the scale unit of TAI approaches the SI second as realised by the ensemble of primary clocks (Azoubib *et al* 1977). TAI is the appropriate reference for illustrating the performance of the individual contributing commercial clocks. Here we present an analysis over a 12-months period, May 2001 to April 2002. Only clocks contributing during the full period have been included. In figure 13a the mean annual rates of 109 clocks of type **A**-H are depicted, the same quantity for the remaining 25 other commercial caesium clocks is given in figure 13b. In principle, the BIPM requests to report un-steered clocks, as delivered from the manufacturer. With a slight reservation, whether this is true in all cases, the plots prove that the clocks in the two ensembles realize the second within the specified accuracy. Another interesting quantity is the instability of the clock ensemble during the 12- months interval, represented by the standard deviation of the monthly rates from the mean. This is depicted in figure 14 for the two clock ensembles.

A final estimate of the averaged relative departure of the TAI scale unit from the SI second is obtained and, to give an example, $8.8 \cdot 10^{-15}$ s was found for the first five months of 2002. The statistically significant deviation is reflected in figure 15 which contains the primary clock data for the last 12 months. Since fountains contribute to the steering of TAI, the uncertainty of the estimate has been reduced to about $2.5 \cdot 10^{-15}$ s. In the future, with inclusion of more fountain data, the accuracy of TAI may further improve. But already today the accuracy and stability of the full clock ensemble (including masers and primary clocks) is effectively transferred to TAI and makes it an excellent reference for time and frequency in scientific applications. TAI is the basis of Coordinated Universal Time UTC, which in turn is the reference for all civil and legal time scales world-wide. UTC differs from TAI only by an integer number of seconds, 32 in mid 2003. This difference increases whenever a leap second is introduced in UTC (Nelson *et al* 2001).

8. The look to the future

Since the mid fifties, when the first caesium atomic clock was successfully operated, the uncertainty in realizing the hyperfine splitting frequency of unperturbed caesium atoms could be reduced by about five orders of magnitude. We can expect some further improvements, but we may also get aware that transitions in other elements prove more suitable in that respect. At present two cold-caesium frequency standards are under development for operation in the micro-gravity environment on the International Space Station (ISS). As T_i only increases proportional to the square-root of the launching height H, there is, for practical reasons, little room for improvement under the action of gravity on Earth. Instead interaction times T_i of 10 s are envisaged in micro-gravity. Of course, the term fountain is no longer adequate as the movement of the atoms will be similar to that in a beam AFS. The standards are named PHARAO (Lemonde *et al* 1999, 2001) and PARCS (Heavner *et al* 2001). Two other projects, GLACE and RACE (Fertig *et al* 1999, 2000) use the element rubidium. PHARAO will become one component of the European Atomic Clock Ensemble in Space (ACES) mission of the European Space Agency (Salomon *et al* 2001) which will also include an active hydrogen maser. ACES was scheduled for flight in 2005 but current policy of NASA regarding the use of the Space Shuttle may lead to a delay. In preparation of the ACES mission, a prototype of the PHARAO standard was tested in the absence of gravity during parabolic flights in an aircraft (Lemonde *et al* 1999, Salomon *et al* 2001). The interaction time T_i could be increased compared to the attainable T_i on Earth at the given size of the PHARAO, proven by recording narrower clock transition Ramsey fringes in the plane than feasible on ground. Meanwhile, the PHARAO prototype has been converted to *La Fontaine Mobile* and was used as a travelling frequency reference (Niering *et al* 2000).

There is room for improvements on ground-based fountain clocks as well. A particular item to be addressed is the collisional frequency shift. Several ways how to minimize it have been proposed or demonstrated. Reduction of the atom number density at a constant *S/N* can be obtained by using more than one cloud of atoms at a time in a fountain (Gibble 1996, Ohshima *et al* 1996, Legere and Gibble 1998). Recently the group at Observatoire Neuchâtel (ON) reported the generation and detection of a continuous low-density atomic beam of slow caesium atoms in a fountain frequency standard, for which the collision shift should be marginally small (Dudle *et al* 2001). The cold-collision shift in fountains could also be reduced by preparing ultra-cold, low density caesium atom clouds and reducing the transversal velocity spread using Raman cooling (Kasevich *et al* 1991). An atom temperature of 150 nK was recently demonstrated, however at the price of a much increased operation complexity (Treutlein *et al* 2001). It appears that a more stable and reproducible frequency standard, though not a realization of the SI second, could be obtained by using ^{87}Rb in

combination with an ultra-stable LO since the collisional shift in ^{87}Rb atoms at the prevailing collisional energies was found to be more than an order of magnitude smaller than for caesium at the same n_{at} (Sortais *et al* 2000, Fertig and Gibble 2000). It is conceivable that the unperturbed hyperfine splitting frequency in ^{87}Rb can be realized with an uncertainty of $1 \cdot 10^{-16}$. It may be difficult to reach this with a caesium fountain.

9. Summary

Currently the definition of the unit of time in the international system of units SI reads "The second is the duration of 9 192 631 770 periods of the radiation corresponding to the transition between the two hyperfine levels of the ground state of the caesium 133 atom.“. The second is the unit which can today be realized with the smallest uncertainty. It is thus quite natural that other base units are defined or realized with reference to it. Since 1983 the meter is a derived unit, defined as the distance travelled by light during 1 / 299 792 s. The realization of the Volt is based on the Josephson effect which couples the units of frequency and voltage through the fundamental constants h (Planck constant) and e (elementary charge). So the second can be regarded as a cornerstone of metrology. Metrology laboratories all over the world realize the unit of time and frequency even if they do not have an obligation to realize and disseminate the legal or official time in their countries (like NMIJ/AIST in Japan or NIST in the US). They either operate primary clocks, subject of Section 5 in this article, or have a means to reference to laboratories that do. Numerous applications of caesium atomic clocks have been identified. Neither satellite based navigation systems, like the US Global Positioning System, nor the syntonization of telecommunication networks at the presently prescribed level would function without them. Thus, there is a substantial market for commercial products, subject of Section 4. There is a future for caesium atomic clocks, in space and on ground, and they will remain useful for scientific and technological applications.

References

Allan D W 1966 Statistics of atomic frequency standards *Proc. IEEE* **54** 221-30

Audoin C 1992 Caesium beam frequency standards: classical and optically pumped *Metrologia* **29** 113-34

Audoin C, Candelier V and Dimarcq N 1991 A limit to the frequency stability of passive frequency standards due to an intermodulation effect *IEEE Trans. Instr. Meas.* **40** 121-5

Audoin C, Santarelli G, Makdissi A and Clairon A 1998 Properties of an oscillator slaved to a periodically interrogated atomic resonator *IEEE Trans. Ultrason. Ferroel. Frequ. Contr.* **45** 877-86

Azoubib J, Granveaud M and Guinot B 1977 Estimation of the scale unit duration of time scales *Metrologia* **13** 87-93

Baldy M L 1996 First commercial prototype of an optically pumped cesium-beam frequency standard *Proc. 28th Annual PTTI Systems and Applications Meeting* pp 281-288

Bassevich A B, Bogdanov P P, Gevorkyan A G and Tyulyakov A E 1996 GLONASS onboard time/frequency standards: ten years of operation *Proc. 28th Annual PTTI Systems and Applications Meeting* pp 455-461

Bauch A and Telle H R 2002 Frequency standards and frequency measurement *Rep. Progr. Phys.* **65** 798-844

Bauch A, Fischer B, Heindorff T, Hetzel P, Petit P, Schröder R and Wolf P 2000 Comparisons of the PTB primary clocks with TAI in 1999 *Metrologia* **37** 683-92

Bauch A, Fischer B, Heindorff T and Schröder R 1998 Performance of the PTB reconstructed primary clock CS1 and an estimate of its current uncertainty *Metrologia* **35** 829-45

Bauch A and Schröder R 1997 Experimental Verification of the Shift of the Cesium Hyperfine Transition Frequency due to Blackbody Radiation *Phys. Rev. Lett.* **78** 622-5

Bauch A and Schröder R 1993 Frequency shifts in a cesium atomic clock due to Majorana transitions *Ann. Physik* **2** 421-49

Bauch A, de Boer H, Fischer B, Heindorff T and Schröder R 1988 Performance of the PTB's Primary Clocks CS2 and CS1 *Proc. 42nd Annual Frequency Control Symp*. pp 490-5

BIPM 1998 *Le Système international d'unités*, 7^{e} édition (Sèvres, France, BIPM)

Boussert B, Cérez P, Chassagne L and Théobald G 1997 Frequency Evaluation of a Miniature Optically Pumped Cesium Beam Clock *Proc. 11th EFTF* pp 58-62

Chu S 1998 The manipulation of neutral particles *Rev. Mod. Phys.* **70** 685-706

Chu S, Hollberg L, Bjorkholm J E, Cable A E and Ashkin A 1985 Three-dimensional viscous confinement and cooling of atoms by resonance radiation pressure *Phys. Rev. Lett.* **55** 48-51

Clairon A, Salomon C, Guellati S and Phillips W D 1991 Ramsey resonance in a Zacharias fountain *Europhys. Lett.* **16** 165-70

Clairon A, Laurent Ph, Santarelli G, Ghezali S, Lea S N and Bahoura M 1995 A cesium fountain frequency standard: preliminary results *IEEE Trans. Instrum. Meas.* **44** 128-31
Clairon A, Ghezali S, Santarelli G, Laurent Ph, Lea S N, Bahoura M, Simon E, Weyers S and Szymaniec K 1996 Preliminary accuracy evaluation of a cesium fountain frequency standard *Proc. 5th Symp. Freq. Standards and Metrology* (Singapore: World Scientific) pp 49–59
Cohen -Tannoudji C N 1998 Manipulating atoms with photons *Rev. Mod. Phys.* **70** 707-20
Cutler L S, Flory C A, Giffard R P and De Marchi A 1991 Frequency pulling by hyperfine σ transitions in cesium beam atomic frequency standards *J. Appl. Phys.* **69** 2780-92
Cutler L S and Giffard R P 1992 Architecture and algorithms for new cesium beam frequency standard electronics *Proc. 1992 IEEE Intern. Frequ. Contr. Symp.* pp 127-33
De Marchi A, Rovera G D and Premoli A 1984 Pulling by neighbouring transitions and its effects on the performance of cesium-beam frequency standards *Metrologia* **20** 37-47
Dick J 1987 Local oscillator induced instabilities in trapped ion frequency standards *Proc. 19th Annual PTTI Systems and Applications Meeting* pp 133-40
Dick J, Prestage J D, Greenhall C A and Maleki L 1990 Local Oscillator Induced Degradation of Medium-Term Stability in Passive Atomic Frequency Standards *Proc. 22nd Annual PTTI Systems and Applications Meeting* pp 487-508
Dudle G, Joyet A, Berthoud P, Mileti G and Thomann P 2001 First results with a cold cesium continuous fountain resonator *IEEE Trans. Instr. Meas.* **50** 510-4
Essen L and Parry J V L 1957 The caesium resonator as a standard of frequency and time *Phil. Trans. Roy. Soc.* **A250** 45-69
Fertig C and Gibble K 2000 Measurement and cancellation of the cold collision frequency shift in an ^{87}Rb fountain clock *Phys. Rev. Lett.* **85** 1622-5
Fertig C, Gibble K, Klipstein B, Kohel J, Maleki L, Seidel D and Thompson R 1999 Laser-cooled microgravity clocks *Proc. 1999 Joint Meet. Europ. Frequ. Time Forum and the IEEE Internat. Frequ. Contr. Symp.* pp 145-7
Fertig C, Gibble K, Klipstein B, Maleki L, Seidel D and Thompson R 2000 RACE: Laser - cooled Rb microgravity clock *Proc. IEEE/EIA Intern. Frequ. Contr. Symp.* pp 676-9
Forman P 1985 Atomichron: the atomic clock from concept to commercial product *Proc. IEEE* **73** 1181-204
Gerber E A and Ballato A 1984 *Precision Frequency Control* (Orlando Fl.: Academic Press)
Gibble K 1996 Collisional effects in cold alkalis *Proc. 5th Symp. Freq. Standards and Metrology* (Singapore: World Scientific) pp 63-73
Hagimoto K, Ohshima S, Nakadan Y and Koga Y 1999 Accuracy Evaluation of the Optically Pumped Cs Frequency Standard at NRLM *IEEE Trans. Inst. Meas.* **48** 496-9

Hasegawa A, Fukuda K, Kajita M, Ito H, Kumagai M, Hosokawa M, Kotake N and Morikawa T 2000 Accuracy evaluation of optically pumped primary frequency standard CRL-01 *Proc. Asia-Pacific Workshop on Time and Frequ.* pp 199-205

Heavner T P, Hollberg L, Jefferts S R, Kitching J, Klipstein W M, Meekhoff D M and Robinson H G 2001 Characterization of a cold cesium source for PARCS: primary atomic reference clock in space *IEEE Trans. Instr. Meas.* **50** 500-2

ISO 1993 G*uide to the Expression of Uncertainty in Measurement*. Geneva: International Organisation for Standardisation

Itano W M, Lewis L L and Wineland D J 1982 Shift of $^2S_{1/2}$ hyperfine splittings due to blackbody radiation *Phys. Rev. A* **25** 1233-5

ITU 1997 *Handbook Selection and Use of Precise Frequency and Time Systems* International Telecommunication Union, Radiocommunication Bureau, Geneva

Jefferts S R, Meekhof D M, Shirley J H, Parker T E and Levi F 1999 Preliminary Accuracy Evaluation of a Cesium Fountain Primary Frequency Standard at NIST *Proc. Joint Mtg. Europ. Freq. Time Forum and the IEEE Int. Freq. Contr. Symp.* pp 12-5

Jones T 2000 *Splitting the Second: The Story of Atomic Time* (Bristol: IOP Publishing)

Kasevich M A, Riis E and Chu S 1989 Rf spectroscopy in an atomic fountain *Phys. Rev. Lett* **63** 612-5

Kramer G 1974 Noise in passive frequency standards *Conference on Precision Electromagnetic Measurement 1974 Conference Digest* 157-9

Kusters J A, Cutler L S and Powers E D 1999 Long-term experience with cesium beam frequency standards *Proc. 1999 Joint Meet. Europ. Frequ. Time Forum and the IEEE Internat. Frequ. Contr. Symp.* pp 159-63

Lee W D, Shirley J H, Lowe J P and Drullinger R E 1995 The accuracy evaluation of NIST-7 *IEEE Trans. Instr. Meas.* **44** 120-3

Lee W D, Drullinger R E, Shirley J H, Nelson C, Jennings D A, Mullen L O, Walls F L, Parker T E, Hasegawa A, Fukuda K, Kotake N, Kajita M and Morikawa T 1999 Accuracy Evaluations and Frequency Comparison of NIST-7 and CRL-01 *Proc. 1999 Joint Meet. Europ. Frequ. Time Forum and the IEEE Internat. Frequ. Contr. Symp.* pp 62-5

Legere R and Gibble K 1998 Quantum scattering in a juggling atomic fountain *Phys. Rev. Lett.* **81** 5780-3

Lemonde P, Laurent Ph, Simon E, Santarelli G, Clairon A, Salomon C, Dimarcq N and Petit P 1999 Test of a space cold atom clock prototype in the absence of gravity *IEEE Trans. Inst. Meas.* **48** 512-4

Lemonde P, Laurent Ph, Santarelli G, Abgrall M, Sortais Y, Bize S, Nicolas C, Zhang S, Clairon A, Dimarcq N, Petit P, Mann A G, Luiten A N, Chang S and Salomon C 2001 Cold-

atom clocks on earth and in space *Frequency measurement and control - Advanced techniques and future trends* (Berlin, Heidelberg, New York: Springer) pp 131-52
Letokhov V S, Ol'shanii M A and Ovchinnikov Yu B 1995 Laser cooling of atoms: a review *Quantum Semiclass. Opt* **7** 5-40
Levine J 1999 Introduction to time and frequency metrology *Rev. Sci. Instr.* **70** 2576-96
Luiten A N, Mann A G, Costa M E, and Blair D G 1995 Power stabilized cryogenic sapphire oscillator *IEEE Trans. Instr. Meas.* **44** 132-5
Lutwak R, Emmons D, Garvey R M, and Vlitas P 2002 Optically pumped caesium-beam frequency standard for GPS-III *Proc. 33rd Annual PTTI Systems and Applications Meeting* pp 19-32
Major F G 1998 *The quantum beat: the physical principles of atomic clocks* (New York, Berlin, Heidelberg: Springer)
Makdissi A and de Clercq E 2001 Evaluation of the accuracy of the optically pumped caesium beam primary frequency standard of the BNM-LPTF *Metrologia* **38** 409-26
Markowitz W, Hall R G, Essen L and Parry J V L 1958 Frequency of cesium in terms of ephemeris time *Phys. Rev. Lett.* **1** 105-7
McCaskill T B, Oaks O J, Largay M M. Reid W G, Warren H E and Buisson J A 1999 Performance of Global Positioning System block II/IIA/IIR on-orbit Navstar clocks *Proc. 31st Annual PTTI Systems and Applications Meeting* pp *75*-89
Meekhoff, D M, Jefferts S R, Stepanovíc M and Parker T E 2001 Accuracy evaluation of a cesium fountain primary frequency standard at NIST *IEEE Trans. Instr. Meas.* **50** 507-9
Metcalf H J and van der Straaten P 1999 *Laser Cooling and Trapping* (New York: Springer)
Naumann R A and Stroke H H 1996 Apparatus upended: a short history of the fountain A-clock *Physics Today* May issue 89-90
Nelson R A, McCarthy D D, Malys S, Levine J, Guinot B, Fliegel H F, Beard R L and Bartholomew T R 2001 The leap second: its history and possible future *Metrologia* **38** 509-29
Nelson L M, Levine J and Hetzel P 2000 Comparing primary frequency standards at NIST and PTB *Proc. IEEE/EIA Intern. Frequ. Contr. Symp.* pp 622-8
Niering M, Holzwarth R, Reichert J, Pokasov P, Udem Th, Weitz M, Hänsch T W, Lemonde P, Santarelli G, Abgrall M, Laurent Ph, Salomon C and Clairon A 2000 Measurement of the hydrogen 1S-2S transition frequency by phase coherent comparison with a microwave cesium fountain clock *Phys. Rev. Lett.* **84** 5496-9
Ohshima S, Kurosu T, Ikegami T and Nakadan Y 1996 Multipulse operation of cesium atomic fountain *Proc. 5th Symp. Freq. Standards and Metrology* (Singapore: World Scientific) pp 60-5

Parker T, Hetzel P, Jefferts S R, Weyers S, Nelson L, Bauch A and Levine J 2001 First Comparison of Remote Cesium Fountains *Proc. 2001 IEEE Frequency Control Symposium* pp 63-8
Parker 2002 NIST, Boulder (US), Time and Frequency Division, private communication
Petit P, Giordano V, Dimarcq N, Cérez P, Audoin C and Théobald G, 1992 Miniature Optically Pumped Cesium Beam Resonator *Proc. 6th EFTF* 1992 pp 83-86
Phillips W D 1998 Laser cooling and trapping of neutral atoms *Rev. Mod. Phys.* **70** 721-41
Raab E L, Prentiss M, Cable A, Chu S and Pritchard D E 1987 Trapping of neutral sodium atoms with radiation pressure *Phys. Rev. Lett.* **59** 2631-4
Ramsey N F 1990 Experiments with separated oscillatory fields and hydrogen masers *Rev. Mod. Phys.* **62** 541-52
Ramsey N F 1950 A molecular beam resonance method with separated oscillating fields *Phys. Rev* **78** 695
Riehle F 2002 *Frequency Standards* (Weinheim: Wiley-VCH)
Salomon C, Dimarcq N, Abgrall M, Clairon A, Laurent P, Lemonde P, Santarelli G, Uhrich P, Bernier L G, Busca G, Jornod A, Thomann P, Samain E, Wolf P, Gonzales F, Guillemot Ph, Leon S, Nouel F, Sirmain Ch and Feltham S 2001 Cold atoms in space and atomic clocks: ACES *C. R. Acad. Sci. Paris*, **Série IV** 1-17
Santarelli G, Audoin C, Makdissi A, Laurent Ph, Dick G J and Clairon A, 1998 Frequency stability degradation of an oscillator slaved to a periodically interrogated atomic resonator *IEEE Trans. Ultrason. Ferreoel. Frequ. Contr.* **45** 887-94
Santarelli G, Laurent Ph, Lemonde P, Clairon A, Mann A G, Chang S, Luiten A N and Salomon C 1999 Quantum projection noise in an atomic fountain: a high stability cesium frequency standard *Phys. Rev. Lett.* **82** 4619-22
Schröder R 1991 Frequency synthesis in primary cesium Clocks *Proceedings 5th European Frequency and Time Forum* pp 194-200
Shirley J, Lee W D and Drullinger R E 2001 The accuracy evaluation of NIST-7 *Metrologia* **38** 427-58
Simon E, Laurent Ph and Clairon A 1998 Measurement of the the Stark shift of the Cs hyperfine splitting in an atomic fountain *Phys. Rev. A* **57** 436-9
Sortais Y, Bize S, Nicolas C, Clairon A, Salomon C and Williams C 2000 Cold collision frequency shifts in a ^{87}Rb atomic fountain *Phys. Rev. Lett.* **85** 3117 - 20
Thomas C and Azoubib J 1996 TAI computation: study of an alternative choice for implementing an upper limit of clock weights *Metrologia* **33** 227-40
Treutlein P, Keng Y C and Chu S 2001 High-brightness atom source for atomic fountains *Phys. Rev. A* **63** 051401(R)

Vanier J and Audoin C 1989 *The Quantum Physics of Atomic Frequency Standards* (Bristol: Hilger)
Weyers S, Bauch A, Schröder R and Tamm Chr. 2002 The atomic caesium fountain CSF1 of PTB 2002 *Proc. 6th Symp. Frequency Standards and Metrology* Ed. P. Gill (Singapore: World Scientific) in press
Weyers S, Hübner U, Fischer B, Schröder R, Tamm Chr and Bauch A 2001 Uncertainty evaluation of the atomic caesium fountain CSF1 of the PTB *Metrologia* **38** 343-52
Wu A and Feess B 2000 Development and evaluation of GPS space clocks for GPSIII and beyond *Proc. 32nd Annual PTTI Systems and Applications Meeting* pp 389 - 99

Figure Captions

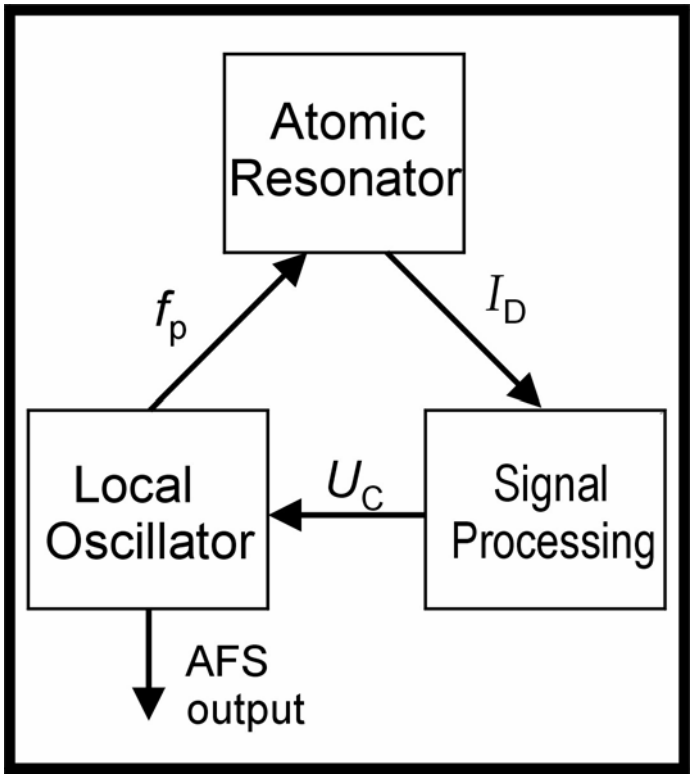

Figure 1. Schematic representation of the function of a *passive* frequency standard in the microwave region. In dependence on the probing frequency f_p, the atomic resonator delivers a response I_D which carries information about the atomic resonance frequency f_r of the probed atomic system. I_D is processed such that f_p on average coincides with f_r. This is achieved by feeding a control signal U_C to the local oscillator delivering standard frequency (5 or 10 MHz) which is fed to a frequency converter (not shown) producing the signal at a frequency f_p close to f_r. This principle of operation applies to the device dealt with in this paper and also to the rubidium gas cell frequency standard, but not to active AFS, like the hydrogen maser, in which the radiation emitted from the atoms is detected; see e. g. Vanier et Audoin (1986).

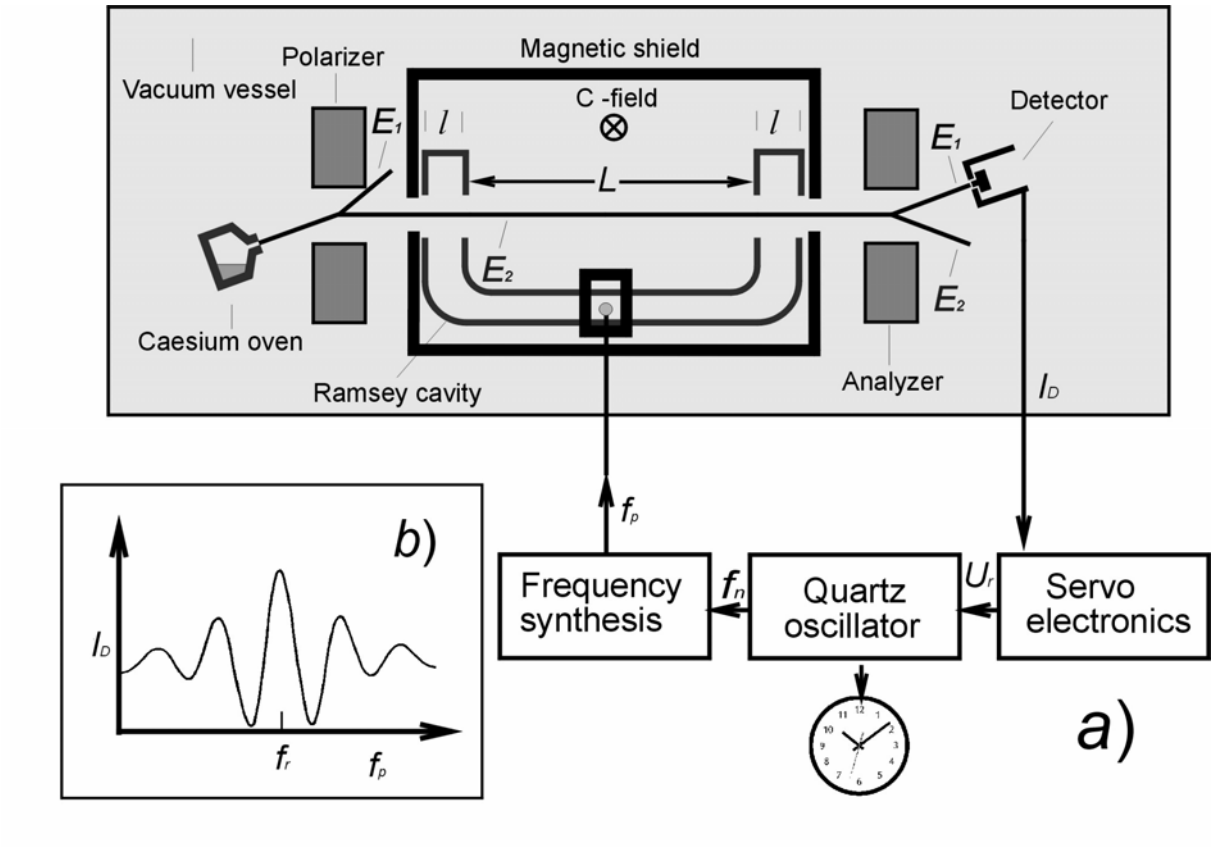

Figure 2. a) Schematic representation of a caesium AFS using magnetic state selection, the function is explained in the text; the grey-shaded rectangle is referred to as caesium beam tube CBT in the text; b) schematic representation of the detected resonance signal when f_p is tuned around f_r. The width of the central resonance feature is inversely proportional to the atoms' averaged time-of-flight through the resonator.

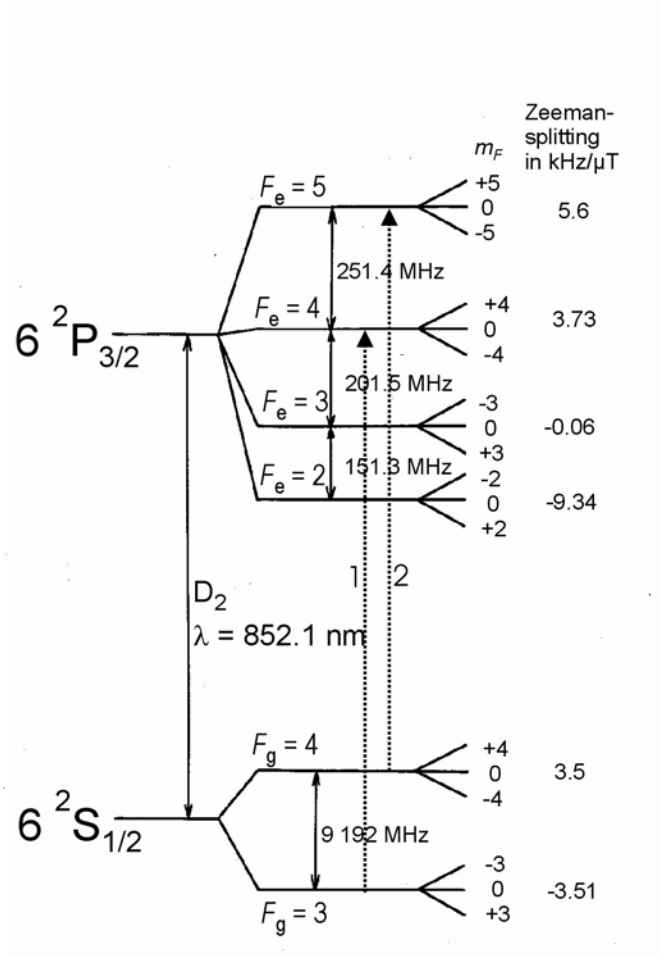

Figure 3. Partial energy level diagram of the ^{133}Cs atom. In high resolution, the two fine structure levels exhibit hyperfine structure (separations of sublevels not to scale). In a small magnetic field (flux density *B*) the hyperfine levels exhibit a linear Zeeman shift proportional to m_F with the indicated frequency shift in kHz per μT of the $m_F = +1$ level. Transition 1 is an example of a so-called pumping transition, used for state-preparation. Transition 2 is a cyclic transition used for detection and for laser cooling of caesium atoms in an atomic fountain (section 6)

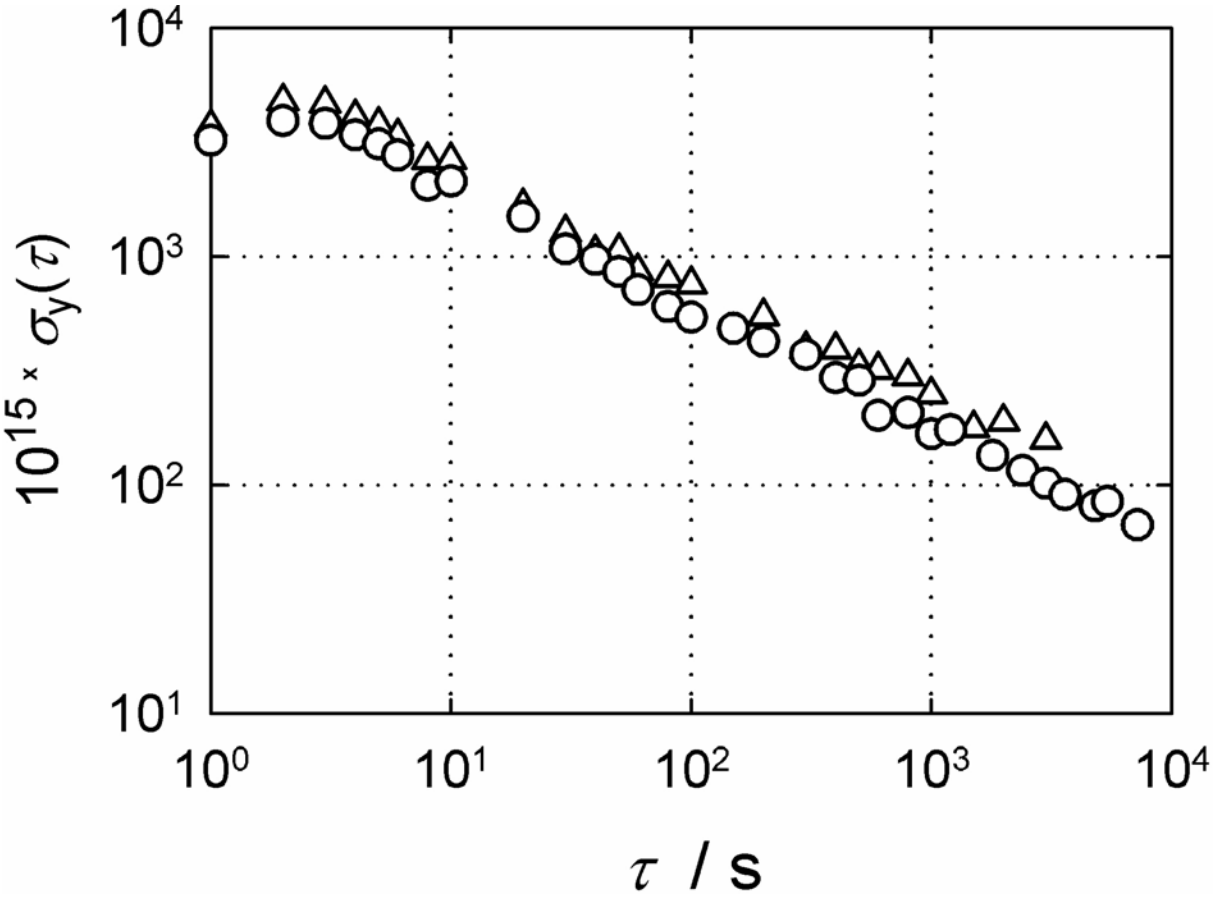

Figure 4. Relative frequency instability $\sigma_y(\tau)$ of a caesium clock **A**-H, serial number 415. An active hydrogen maser was used as reference clock and a high resolution phase comparator was used for the measurement. Thus the data reflect the clock instability only. Data (Δ) were taken in the fifth year of operation of the CBT, data (O) were taken immediately when a new CBT had just been installed.

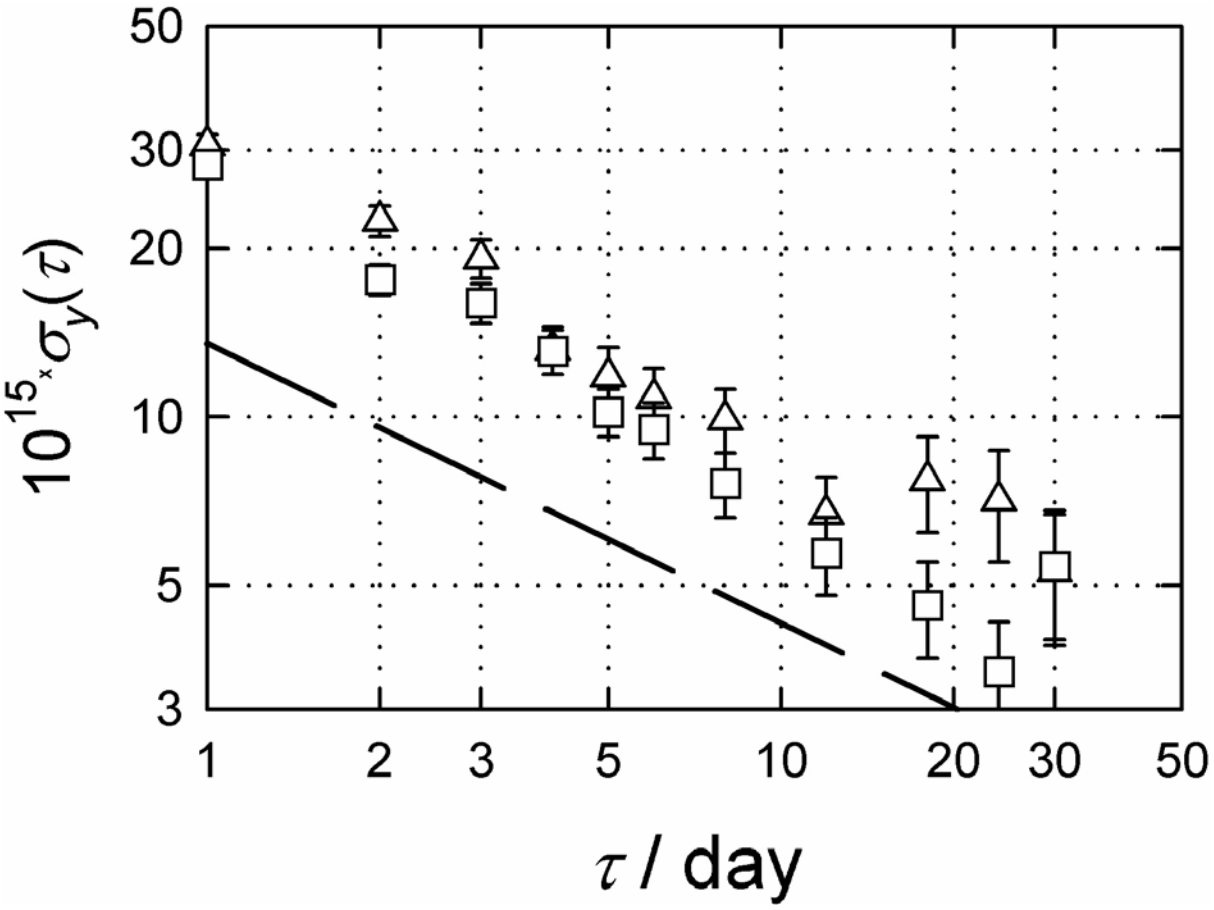

Figure 5 Relative frequency instability $\sigma_y(\tau)$ of two caesium clock **A**-H, serial numbers 128 (Δ) and 415 (□), 360 days of data up to 30th April 2002. UTC(PTB) served as reference and a high-resolution time interval counter was used for the measurement. The dashed line indicates the lowest possible instability to be determined with the given measurement set-up, limited by white frequency noise of PTB's primary clock CS2 which serves as source of UTC(PTB) (Bauch *et al* 2000).

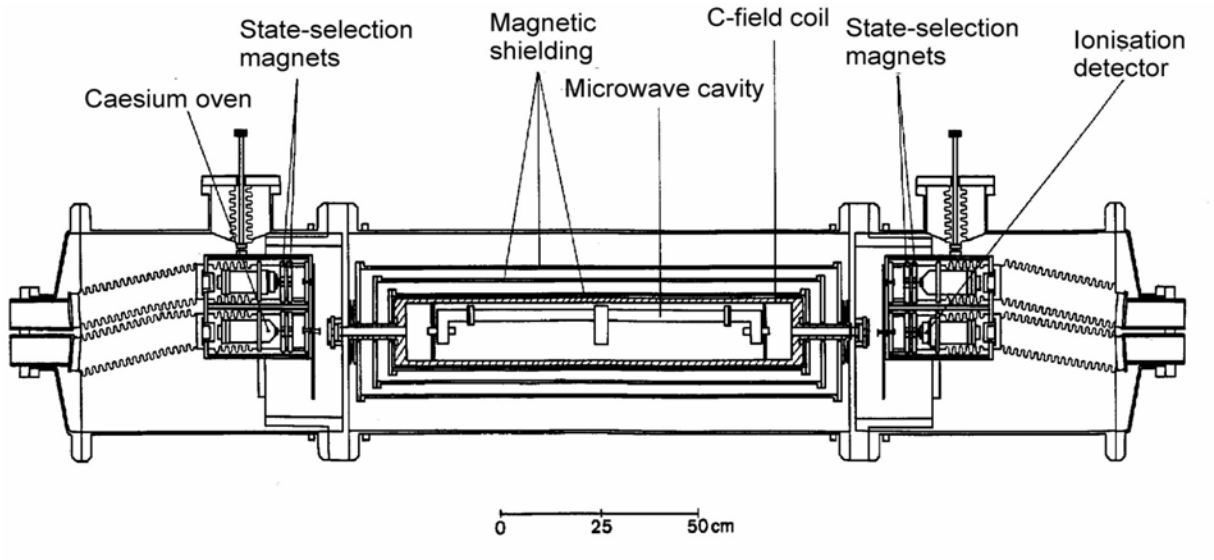

Figure 6. Vertical section of the vacuum chamber of PTB's primary clock CS2. The constituent elements are explained in section 3. An oven and detector at each end allows alternate operation of atomic beams in opposite directions without disturbing the vacuum conditions.

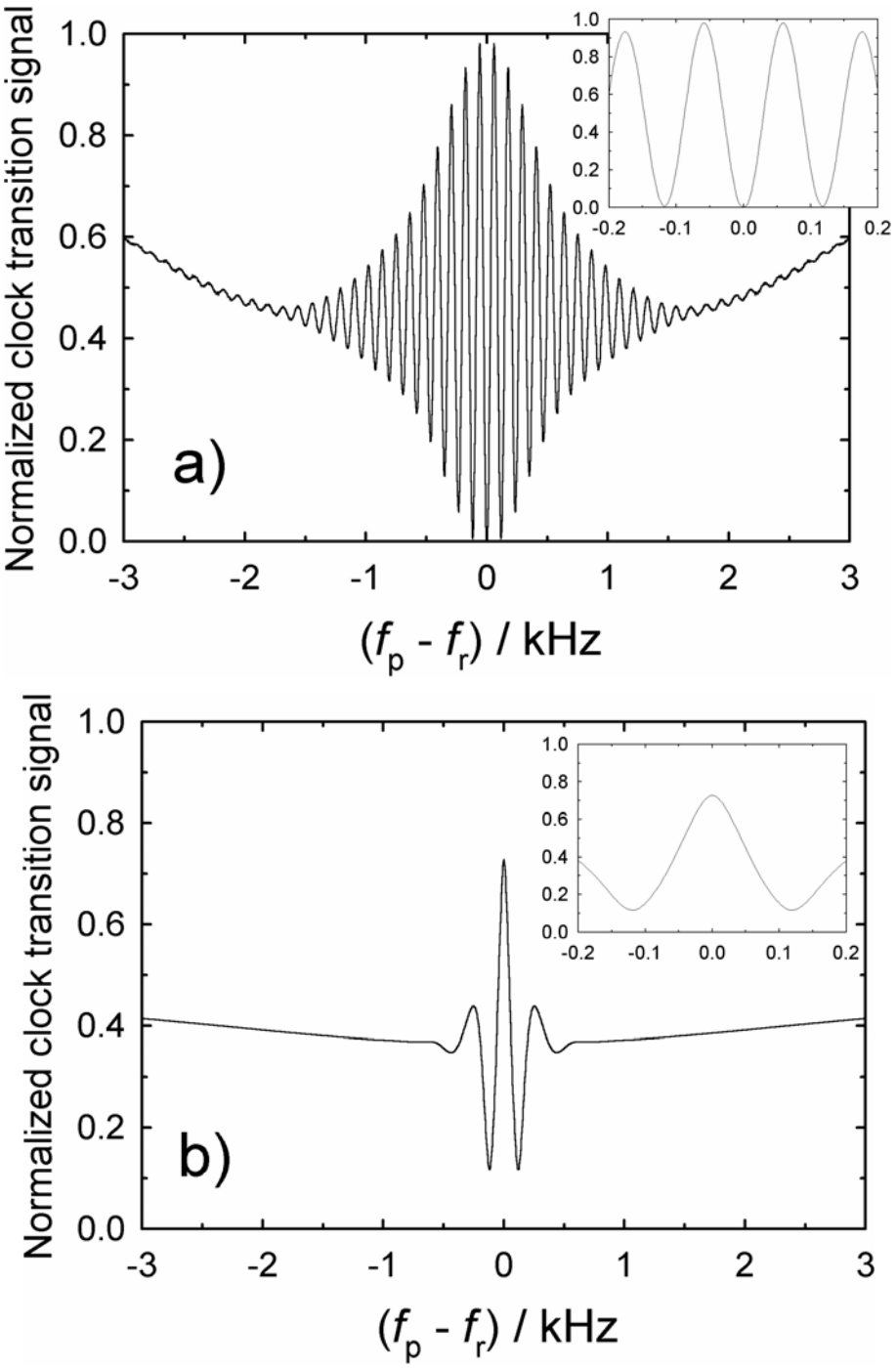

Figure 7. Records of the (F_g=4, m_F = 0)→(F_g = 3, m_F = 0) clock transition at f_r = 9 192 MHz (inserts: central fringes in higher resolution); the signals represent ensemble velocity averages of the transition probability between the m_F = 0 hyperfine ground-state energy levels; a) record from PTB's primary clock CS2. In CS2, the atoms that made the clock transition to the F_g=3 state are deflected from the detector, so that I_D shows a minimum in resonance; b) record from the French primary clock JPO using optical pumping. Here I_D shows a maximum in resonance as optical detection is sensitive to the atoms which made a transition; the JPO data file was made available by A. Makdissi, LPTF.

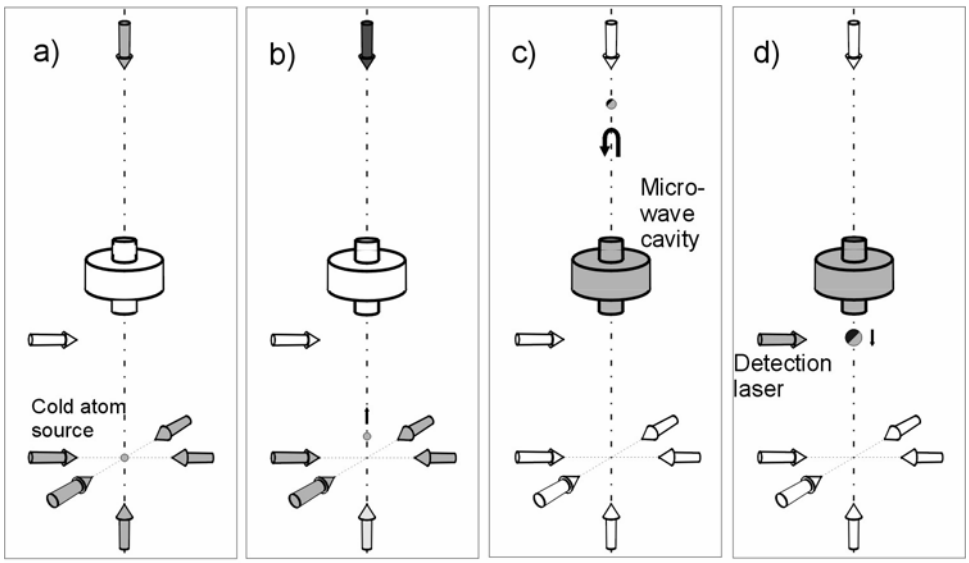

Figure 8. Sequence of operation of a fountain frequency standard, illustrated in a time sequence from left to right; laser beams are indicated by arrows (white if they are blocked). a) A cloud of cold atoms is loaded. b) The cloud is launched by de-tuning of the frequency of the vertical lasers. c) The cloud with an initially small volume and high density expands during ballistic flight. d) After the second passage of the atoms through the cavity the state population is probed by laser irradiation and fluorescence detection.

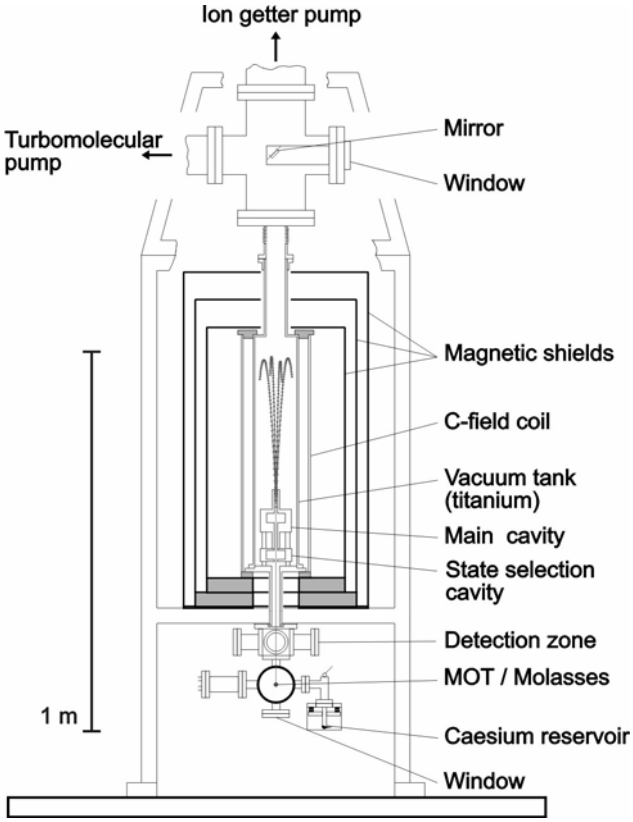

Figure 9. Schematic drawing of the vacuum chamber of the PTB caesium fountain CSF1

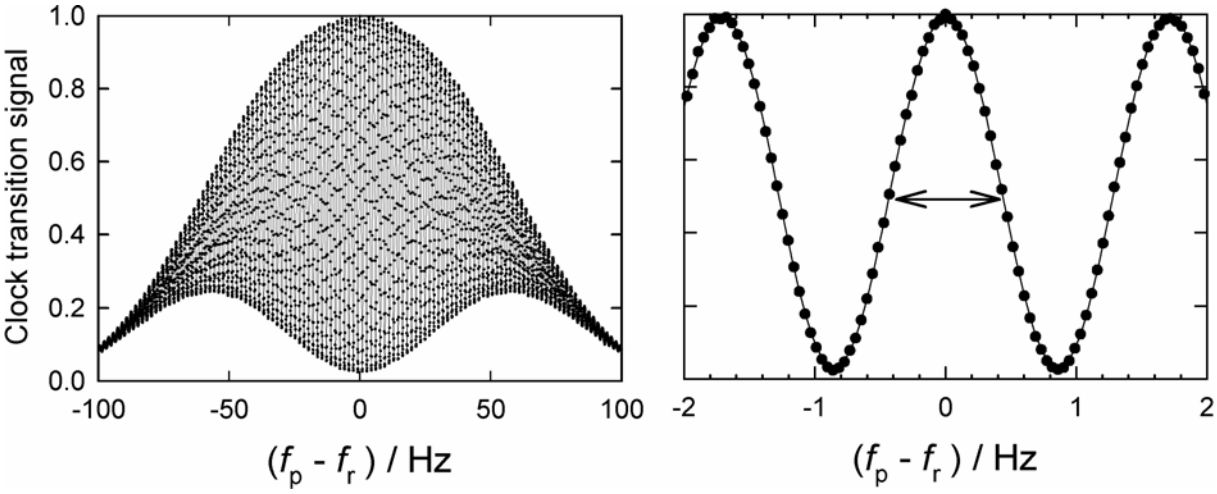

Figure 10. Record of the (F=4, m_F=0) - (F=3, m_F=0) clock transition in the PTB CSF1. Each dot represents the outcome of one fountain cycle, the probing frequency is incremented after each cycle. The connecting lines help to recognise the pattern; right plot: high resolution record of the central fringes. During frequency measurement, f_p is modulated as indicated by the arrow.

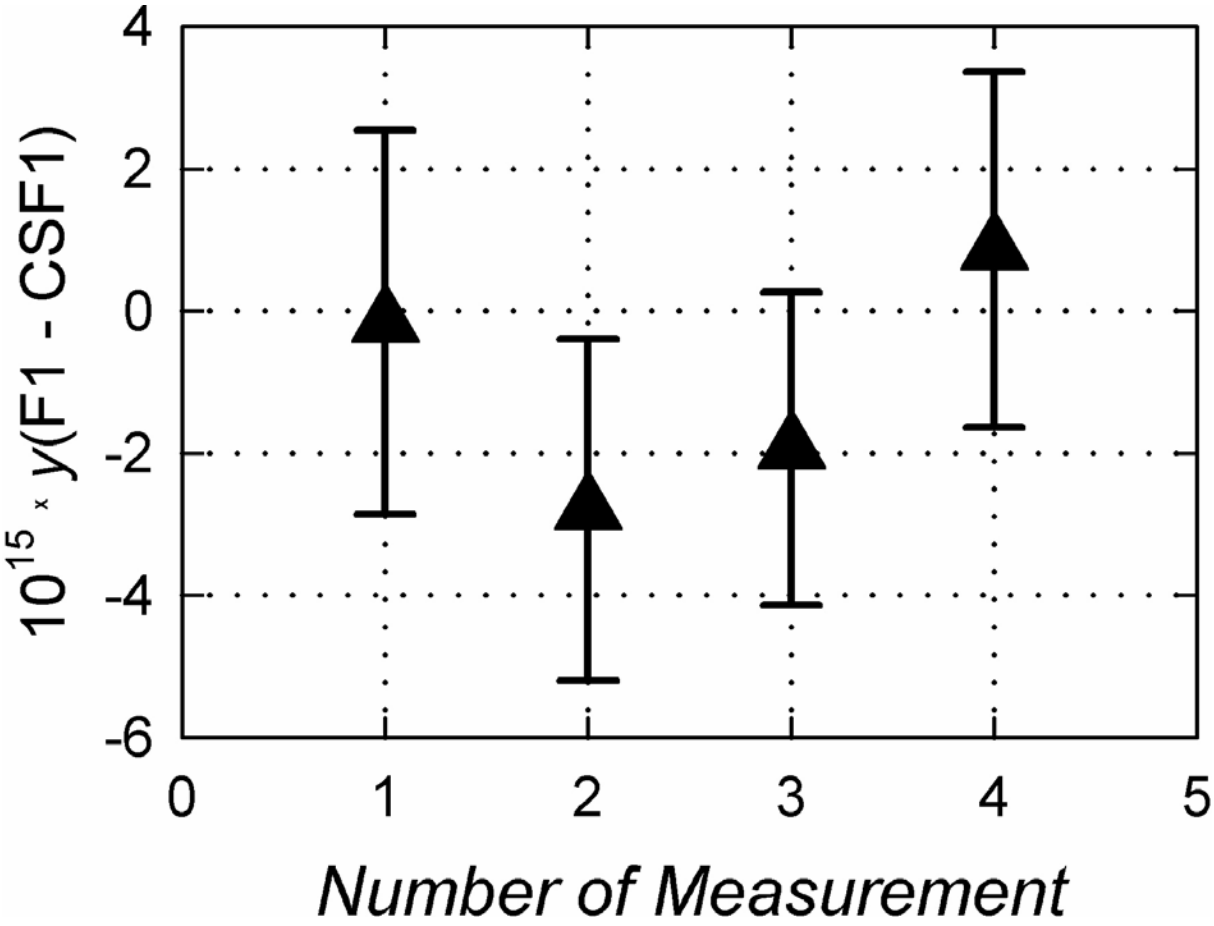

Figure 11. Relative frequency difference between NIST-F1 and PTB CSF1 (Parker *et al* 2001, Parker 2002); "error bars" reflect the combined uncertainty due to the u_B values of both fountains and the measurement uncertainty. The comparisons took place in August 2000, July 2001, November 2001 and February 2002.

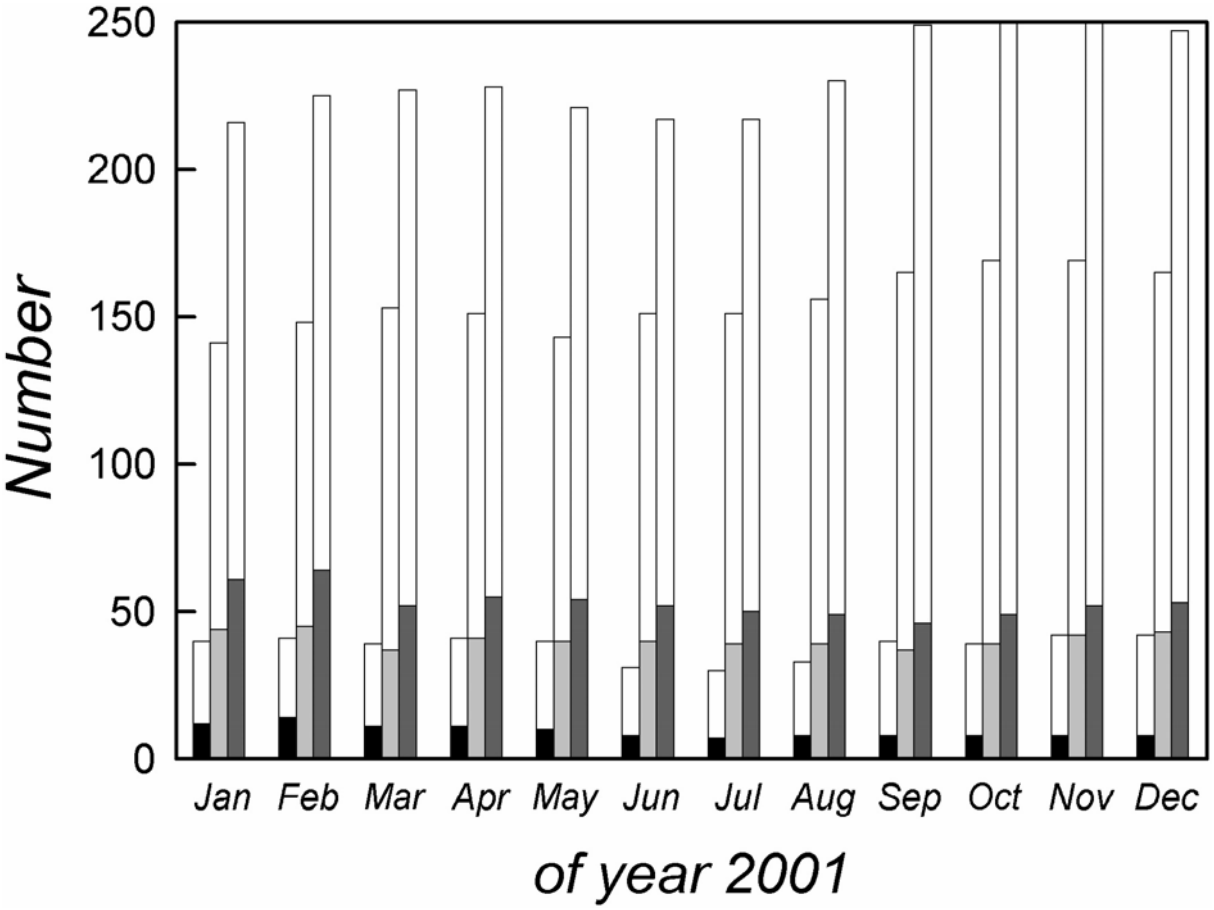

Figure 12. Number of clocks contributing to the realization of EAL in 2001. For each month of 2001, a triple of bars indicates the number of hydrogen masers (left), of clocks of type **A**-H (see Table 2) (middle), and the total number (right). In grey shade the fraction of these clocks having been attributed the maximum statistical weight is indicated. One notices that the clocks of type **A**-H make up the largest fraction of clocks having obtained maximum weight. Source: file wtai01.ar in directory pub/tai/scale of the BIPM Time Section.

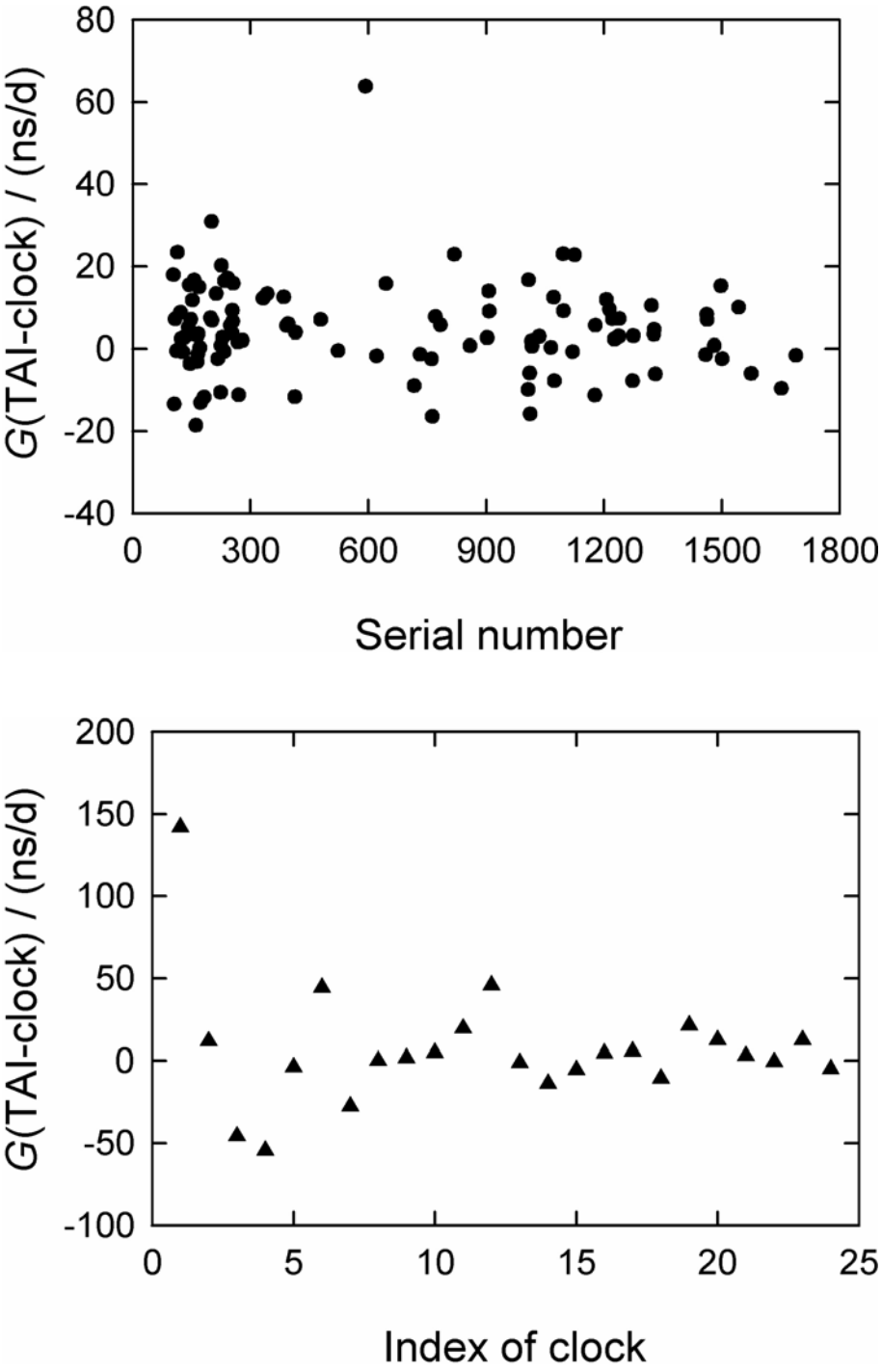

Figure 13. Mean annual rate of 109 individual clocks contributing to the realization of EAL during the 12-month period May 2001 – April 2002, expressed in ns/d (a rate of 0.86 ns/d corresponds to a relative frequency deviation of $1 \cdot 10^{-14}$); a) clocks of type **A**-H (see Table 2) , plotted against their serial number; b) commercial caesium clocks others than those in a) plotted in sequence of their introduction in BIPM files. Source: files r01.10 and r02.04 in directory pub/tai/publication of the BIPM Time Section.

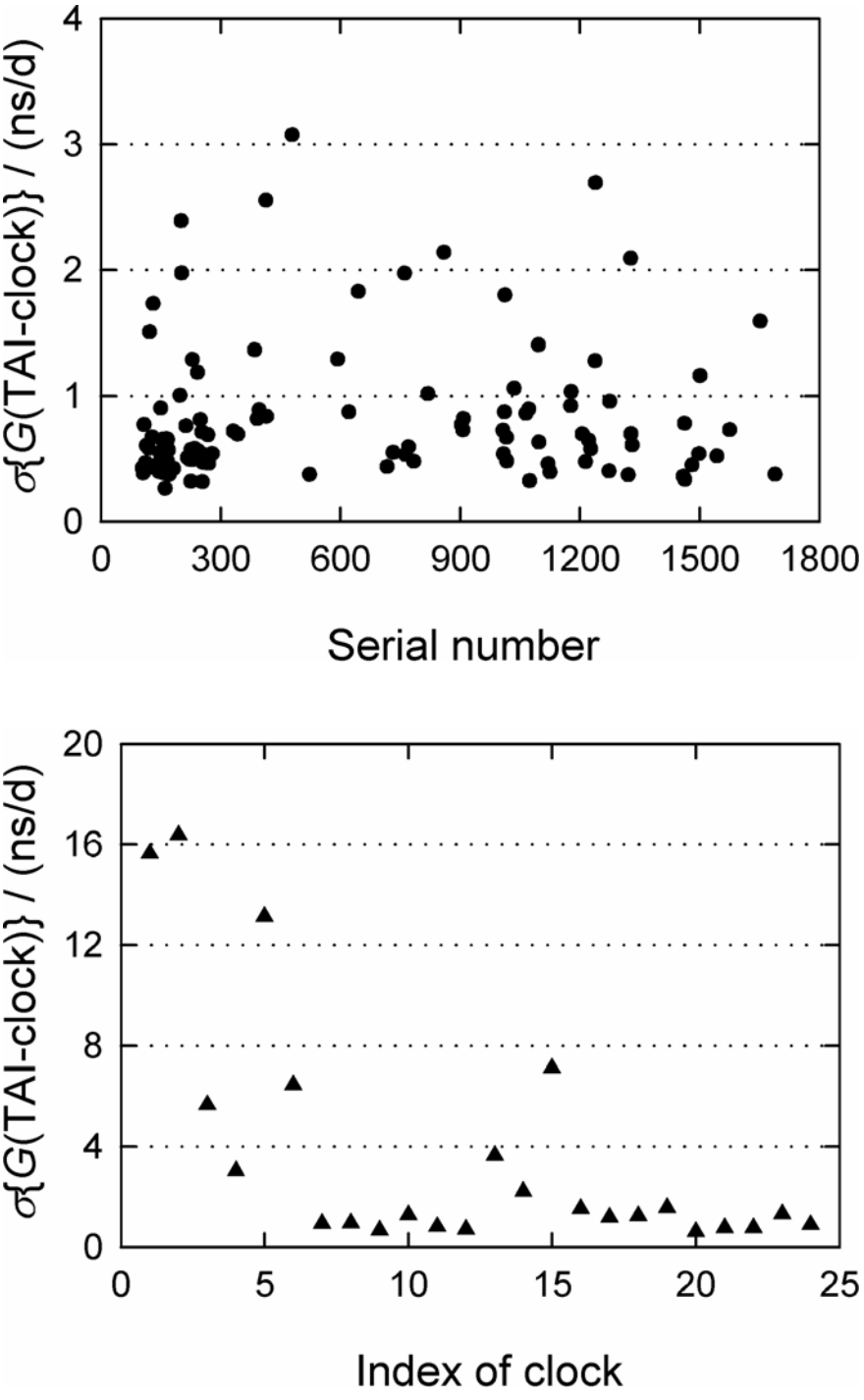

Figure 14. Standard deviation of the 12 monthly rates around the respective annual mean va

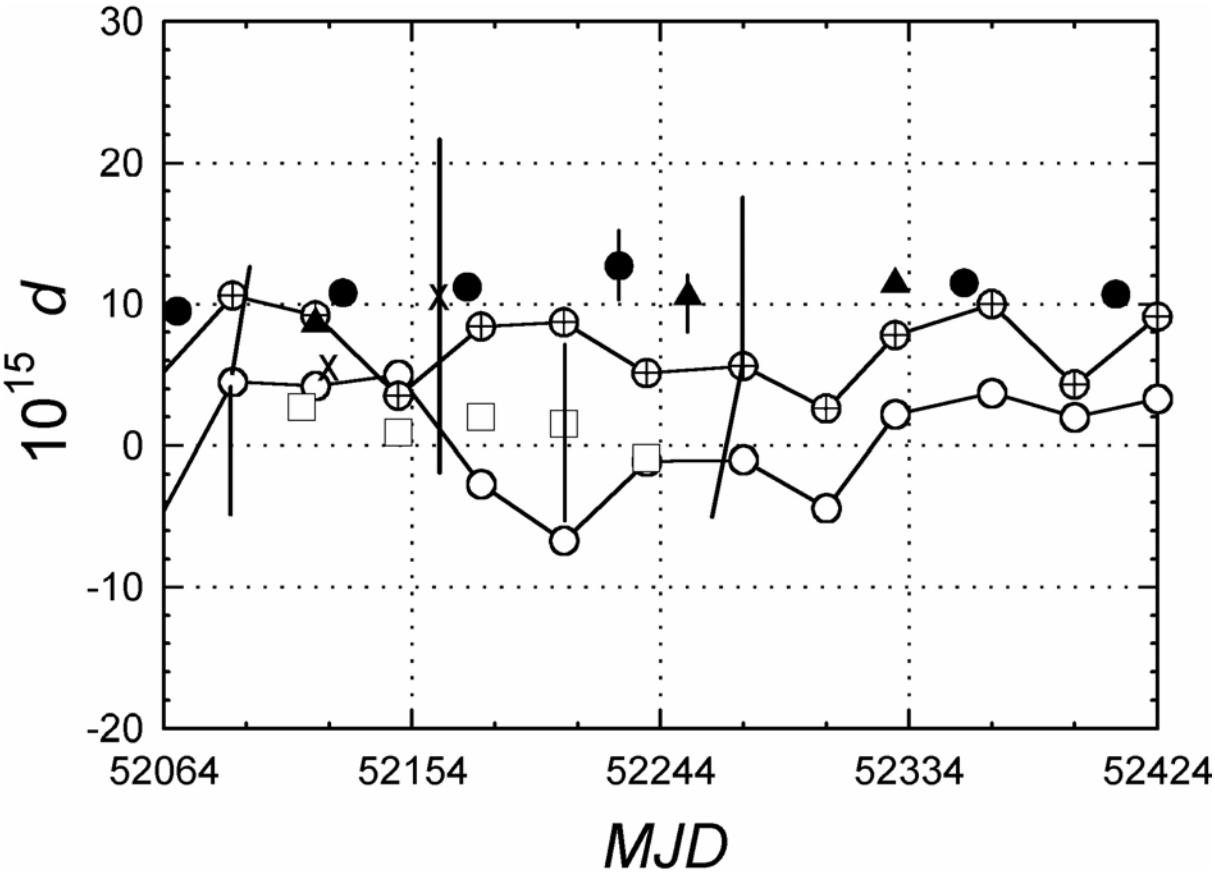

Figure 15. Fractional deviation *d* of the duration of the TAI scale interval from the SI second as realized by the individual primary clocks CSF1 (•), CS1 (O) and CS2 (⊕) of PTB, NIST-F1 (▲), CRL-01 (X) (Japan), and JPO (□) (France) during the period MJD 52064 - 52424. MJD designates the Modified Julian Date; MJD 52424 corresponds to 30th May 2002. Data points from PTB's CS1 and CS2 were connected to indicate continuous operation. For the other clocks the symbols are plotted at the end of the measurement intervals of a duration between 15 and 35 days. "Error bars" (one representative for each clock) indicate the 1σ - standard uncertainty in the determination of *d.*

Table Caption

Table 1 Manufacturers of commercial caesium clocks, including a point of contact and a single character acronym used throughout sections 4 and 7. The Physikalisch-Technische Bundesanstalt as a matter of policy does not endorse any commercial product. The mentioning of brands and individual models seems justified here, because all information provided is based on publicly available material or data taken at PTB and it will help the reader to make comparison with own observations.

Table 2. Specifications of caesium AFS of the manufacturers **A** and **D**. The information was taken from latest sales brochures and from the companies' points of contact. n.s.: not specified. Manufacturer **A** specifies that the relative clock frequency remains unchanged within $1 \cdot 10^{-13}$ for the standard model and $8 \cdot 10^{-14}$ for the high performance model for the full range of specified environmental changes: magnetic flux density (DC, 50 Hz, 60 Hz) up to 0.2 mT, temperature between 0 °C and 50 °C, relative humidity between 0% and 80%. Manufacturer **D** specifies for the most recent CS III product line a similar range of operating conditions. At a applied magnetic field of 0,2 mT flux density, the relative AFS frequency does not change by more than $2 \cdot 10^{-14}$. Temperature sensitivity is reported as < 1.2 10^{-13} / °C for the CS III standard option and < $1.2 \cdot 10^{-14}$ /°C for the high performance option.

Table 3. Line quality factor Q, and relative frequency instability $\sigma_y(\tau = 1\ \mathrm{s})$ of the five primary frequency standards with a thermal beam discussed in the text. Data were taken from the references describing the standards.

Table 4. Uncertainty budgets of the five primary clocks with a thermal beam in parts in 10^{15}, cited in the text. "0" indicates that the component is not of relevance at all. It is common practise to calculate the combined uncertainty as the root-sum-of squares of the individual components, assuming that they are linearly independent. It has the meaning that the duration of the realized second intervals agrees with the defined duration within $\pm u$ with about two-thirds probability.

Table 5. Uncertainty contributions in parts in 10^{15} of the three caesium fountain frequency standards cited in the text. "<0.1" indicates that the component is by all means smaller than 10^{-16} or not considered of relevance by the authors, Lemonde *et al* (2001) for FO1, and Weyers *et al* (2001) for CSF1. For NIST-F1 the most recent data are given, valid for a 25-day period in February 2002 (Parker 2002).

Table 1

Agilent Technologies	www.agilent.com	**A**
Datum - Timing, Test &Measurement (part of Symmetricom since beginning of 2003)	www.datum.com www.symmetricom.com	**D**
Frequency Electronics, Inc.	www.fei.com	**F**
Kernco, Inc.	www.kernco.com	**K**
Oscilloquartz SA	www.oscilloquartz.com	**O**

Table 3

Quantity to characterize the performance	**JPO**	**NIST-7 (CRl-01)**	**NRLM-4**	**CS1**	**CS2**
Line quality factor $Q/10^8$	1	1.6	1.2	1.6	1.6
Rel. frequency instability $10^{13}\cdot\sigma_y(\tau=1s)$	2.9	7	8	55	36

Table 4

Cause of frequency shift	JPO	NIST-7 (CRl-01)	NRLM-4	CS1	CS2
Quadratic Zeeman effect	1.3	1	10	1	5
Quadratic Doppler effect	2.6	3	3	1	1
AC Stark effect caused by thermal radiation	0.5	1	1	1	1
Cavity phase difference	4	4	23	6	10
Detuning of the microwave cavity	0.4	1	8	0.3	0.1
AC Stark effect caused by fluorescence-radiation	2.4	1	10	0	0
Asymmetric population of the Zeeman sublevels	2.3	1	7	0.2	0.1
Electronics	2	3	1	1	3

Table 5

Cause of frequency shift	**LPTF FO1**	**NIST- F1**	**PTB-CSF1**
Quadratic Zeeman effect	<0.1	< 0.1	< 0.1
Quadratic Doppler effect	<0.1	< 0.1	< 0.1
AC Stark effect caused by thermal radiation	0.5	0.3	0.2
Cavity phase difference (distributed)	0.5	<0.1	0.5
Detuning of the microwave cavity	0.1	<0.1	<0.1
AC Stark effect caused by fluorescence-radiation	<0.1	0.2	0.2
Asymmetric population of the Zeeman sublevels	0.4	<0.1	< 0.1
Cold atom collisions	0.5	0.48	0.7
Electronics	0.3	0.2	0.2

Diese Seite enthält weiter keinen Text.

Table 2

clock type	**A** 5071 Standard (**A**-S)	**A** 5071 High Performance (**A**-H)	**D**-4065 Standard	**D**-4065 High performance	**D**-4040 B Standard	**D**-4040 B High performance	**D**- CS III Standard	**D**-CS III High performance
Accuracy	$1\cdot10^{-12}$	$5\cdot10^{-13}$	$1\cdot10^{-12}$	$5\cdot10^{-13}$	$< 2\cdot10^{-12}$	$< 1\cdot10^{-12}$	$2\cdot10^{-12}$	$5\cdot10^{-13}$
$\sigma_y(\tau = 100s)$	$< 2.7\cdot10^{-12}$	$<8.5\cdot10^{-13}$	$< 2.7\cdot10^{-12}$	$< 8.5\cdot10^{-13}$	$< 5\cdot10^{-12}$	$<8.5\cdot10^{-13}$	$<2.7\cdot10^{-12}$	$8.5\cdot10^{-13}$
minimum σ_y, guaranteed typical result	$<5\cdot10^{-14}$ $<1.5\cdot10^{-14}$	$<1\cdot10^{-14}$ $<5\cdot10^{-15}$	$< 5\cdot10^{-14}$	$< 1\cdot10^{-14}$	$<8\cdot10^{-14}$	$<2\cdot10^{-14}$	$<5\cdot10^{-14}$	$< 2\cdot10^{-14}$
special features	see caption	see caption	9 rf outputs	9 rf outputs	4 rf outputs	4 rf outputs	see caption compact lightweight (13.5 kg)	see caption compact lightweight (13.5 kg)
Warranty	electr. 1 y tube 10 y	electr. 1 y tube 3 y	electr. 2 y tube 12 y	electr. 2 y tube 12 y	n.s.	n.s	n.s	n.s